JOURNAL OF GEOPHYSICAL RESEARCH, VOL. 94, NO. D14, PAGES 16,683–16,703, NOVEMBER 30, 1989

Nitrogen and Chlorine Species in the Spring Antarctic Stratosphere: Comparison of Models With Airborne Antarctic Ozone Experiment Observations

J. M. RODRIGUEZ,[1] M. K. W. KO,[1] N. D. SZE,[1] S. D. PIERCE,[1] J. G. ANDERSON,[2]
D. W. FAHEY,[3] K. KELLY,[3] C. B. FARMER,[4] G. C. TOON,[4] M. T. COFFEY,[5]
L. E. HEIDT,[5] W. G. MANKIN,[5] K. R. CHAN,[6] W. L. STARR,[6]
J. F. VEDDER,[6] AND M. P. MCCORMICK[7]

The Atmospheric and Environmental Research, Inc., photochemical model has been used to simulate the concentrations and time development of key trace gases in the Antarctic stratosphere before, during, and after the Airborne Antarctic Ozone Experiment (AAOE). The model includes complete gas phase photochemistry and heterogeneous reactions of $ClNO_3$ (g) and N_2O_5 (g) with HCl (s) and H_2O (s). Observations of long-lived species by the AAOE instruments have been used to constrain the initial conditions in our calculations. We present results from four cases illustrating the evolution of the trace gases for a range of possible initial conditions and duration of heterogeneous activity. The amount of ClO produced by heterogeneous conversion of HCl is determined not only by the initial concentrations of NO_x ($NO + NO_2 + NO_3$), N_2O_5, and $ClNO_3$ during winter, but also by the rate at which NO_x is resupplied by photolysis of N_2O_5 and HNO_3, or by transport. Results from the four cases presented bracket column measurements of HCl, $ClNO_3$, and HNO_3 by the Jet Propulsion Laboratory and National Center for Atmospheric Research infrared spectrometers onboard the NASA DC-8, and in situ measurements of ClO and NO_y by instruments aboard the NASA ER-2. Comparison of results and measurements of HCl and ClO suggests that heterogeneous chemistry was maintained throughout the month of September in 1987. We suggest field observations and kinetic data which would further constrain the photochemistry of the spring Antarctic stratosphere. The behavior of ozone is discussed in a companion paper (Ko et al., this issue).

1. INTRODUCTION

The unusual behavior of ozone during Antarctic spring has elicited great interest from both the scientific community and the general public during the past 3 years. The decrease in ozone was first pointed out by *Farman et al.* [1985] from their analysis of ground-based observations by the British Antarctic Survey station at Halley Bay. Subsequent analysis of ground-based measurements at other stations [*Chubachi*, 1986; *Bojkov*, 1986], of satellite data [*Stolarski et al.*, 1986; *Krueger et al.*, 1987] and of balloon measurements [*Chubachi*, 1984; *Hofmann et al.*, 1986, 1987] has established beyond doubt the existence and extent of the so-called "ozone hole" during Antarctic spring, and the decreasing trend of the October minimum values during the past 10 years. These observations have greatly intensified research activities in stratospheric ozone and led to a reevaluation of recent ozone trends at other latitudes [*NASA*, 1988].

The first National Ozone Expedition (NOZE I) conducted ground-based and balloon measurements from McMurdo station, Antarctica, during the austral spring of 1986. Balloon measurements from this campaign confirmed the occurrence of large depletions of ozone between 12 and 20 km, often exhibiting a layered structure [*Hofmann et al.*, 1987]. Measurements of the column abundances of ClO, OClO, NO_2, NO, HNO_3, HCl, and $ClNO_3$ indicated a highly perturbed chemical composition, unlike any other environment on Earth. In particular, concentrations of ClO and OClO were about a factor of 100 higher than predicted by models [*P. Solomon et al.*, 1987; *de Zafra et al.*, 1987; *S. Solomon et al.*, 1987], while column abundances of NO_2, HCl, and HNO_3 were considerably reduced [*Mount et al.*, 1987; *Farmer et al.*, 1987]. Column densities of $ClNO_3$ as high as 4×10^{15} cm^{-2} were observed by the Jet Propulsion Laboratory (JPL) infrared spectrometer [*Farmer et al.*, 1987], giving an [HCl]/[$ClNO_3$] of 0.5–0.3 (mid-latitude values are of order 4). Recent values for OClO, ClO, and NO_2 from the 1987 NOZE II campaign confirm the 1986 results [*Sanders et al.*, 1989; *Solomon et al.*, 1989; *de Zafra et al.*, 1989].

This paper examines the constraints placed by Airborne Antarctic Ozone Experiment (AAOE) observations of chlorine and nitrogen species on current photochemical theories of the Antarctic ozone phenomenon, particularly those involving chlorine-related mechanisms. Data from AAOE are used in two ways: (1) measurements of long-lived species such as CH_4 are adopted as input to the model calculations, and (2) observations of concentrations and temporal behavior of short-lived species such as ClO are compared with model results to provide constraints for different scenarios. Our modeling study is intended to address the following questions: (1) how does the partitioning of chlorine species depend on the rates of different heterogeneous mechanisms, and on the concentrations of chlorine and nitrogen species prior to the onset of heterogeneous chemistry?, (2) what are the rates and duration of heterogeneous mechanisms re-

[1]Atmospheric and Environmental Research, Inc., Cambridge, Massachusetts.
[2]Harvard University, Cambridge, Massachusetts.
[3]NOAA Aeronomy Laboratory, Boulder, Colorado.
[4]Jet Propulsion Laboratory, Pasadena, California.
[5]National Center for Atmospheric Research, Boulder, Colorado.
[6]NASA Ames Research Center, Moffett Field, California.
[7]NASA Langley Research Center, Hampton, Virginia.

Paper number 89JD00854.
0148-0227/89/89JD-00854$05.00

quired to explain the observed concentrations and temporal behavior of trace gases in the stratosphere during Antarctic spring?, and (3) what is the expected temporal development of stratospheric trace gases before and after the period covered by the AAOE campaign? Two additional questions will be addressed in a companion paper [*Ko et al.*, this issue]: (4) do catalytic cycles involving chlorine species account for the observed reductions in O_3, both during and after the AAOE period?, and (5) can chlorine chemistry solely explain the sudden onset of the antarctic ozone hole in the late 1970s, and its rapid deepening during the past decade?

Previous studies have addressed some of the above questions, based on the observed column densities of NO, NO_2, HCl, HNO_3, $ClNO_3$, and ClO observed during NOZE I at McMurdo. *McElroy et al.* [1988] simulated enhanced abundances of ClO and large decreases in O_3 in the absence of any heterogeneous chemistry after mid-August by assuming that about half of the nitric acid below 20 km was removed by particle deposition, thus emphasizing the role of denitrification in Antarctic chemistry. Their results indicate that substantial amounts of HNO_3 must be left in the gas phase, however, in order to provide sufficient NO_x to account for the large column densities of $ClNO_3$ observed by the JPL infrared spectrometer during the 1986 austral spring [*Farmer et al.*, 1987]. *Wofsy et al.* [1988] have pointed out that the abundance of nitrogen oxides in the winter Antarctic stratosphere may play an important role in controlling the amount of active chlorine ($Cl + ClO + 2 \times Cl_2 + 2 \times Cl_2O_2 + OClO + HOCl$) produced by heterogeneous conversion of HCl and, in particular, could explain the deepening of the ozone hole observed since the mid-1970s. The actual concentrations of NO_x ($NO + NO_2 + NO_3$) during polar winter are uncertain, thus allowing for a range of possibilities in the partitioning of ClO_x (active chlorine + $ClNO_3$). *Salawitch et al.* [1988] have suggested that ozone reductions in a particular year will be controlled by the fraction of HNO_3 permanently removed by denitrification.

The above suggestions can now be tested in the context of the measurements by the AAOE instruments. Observations of $ClNO_3$ in early September can shed light on the initial nitrogen oxide concentrations prior to heterogeneous processing. Measurements of column HNO_3 and in situ NOY place constraints on the amount of nitric acid left in the gas phase. Analysis of HCl and ClO observations in conjunction with photochemical models can place important constraints on the duration of heterogeneous processes. Photochemical models constrained by the above data can then be used to extrapolate the behavior of trace gases to times not covered by the AAOE, i.e., early August, October, or years before and after 1987.

We present results of four plausible, although not exhaustive, scenarios adopting different initial conditions and temporal behavior of heterogeneous reactions. Results of these scenarios bracket observations from AAOE. We will argue that comparison of our results with AAOE observations suggests that heterogeneous chemistry played an important role during most of September in 1987. Comparison of calculations and observations will also identify kinetic data and observations needed to further constrain the behavior of trace gases before and after the AAOE period, and resolve remaining uncertainties in chlorine-related theories of the Antarctic ozone hole.

Section 2 presents a brief summary of the chlorine-related hypotheses of the Antarctic ozone hole phenomenon and the present knowledge of the heterogeneous mechanisms invoked by these hypotheses. The conversion of HCl by heterogeneous chemistry and its sensitivity to the abundance of nitrogen oxides are discussed in section 3. Our modeling approach, calculations, and choice of scenarios are discussed in section 4. Results of our calculations are discussed in conjunction with AAOE observations in section 5. The main conclusions of the study are summarized in section 6.

2. Chlorine Hypotheses and Heterogeneous Chemistry

Early attempts to explain the "ozone hole" invoked either chemical or dynamical processes. Dynamical theories have proposed a reverse circulation with upward motions during Antarctic spring to explain part of the O_3 seasonal decrease [*Tung et al.*, 1986]. The interannual trend has been attributed in these theories to a decrease in planetary wave activity and meridional transport of ozone during the last decade [*Mahlman and Fels*, 1986]. Chemical hypotheses have suggested enhanced catalytic removal of ozone due to either very high abundances of NO_2 [*Callis and Natarajan*, 1986] or of active chlorine species [*Solomon et al.*, 1986; *McElroy et al.*, 1986*a*; *Molina and Molina*, 1987] during Antarctic spring. Measurements of NO_2 during the NOZE I and NOZE II campaigns [*Mount et al.*, 1987; *Farmer et al.*, 1987]; and during the AAOE campaign [*Toon et al.*, this issue; *Wahner et al.*, this issue] rule out a significant contribution by NO_2-related cycles to the observed ozone reductions. Assessment of the role of dynamics in the ozone hole phenomenon is discussed by, among others, *Tuck* [1989] and *Hartmann et al.* [this issue].

Chlorine-related theories invoke the following cycles for removing ozone [*Solomon et al.*, 1986; *McElroy et al.*, 1986*a*; *Molina and Molina*, 1987]:

Cycle I

$$Cl + O_3 \rightarrow ClO + O_2 \quad (1)$$

$$OH + O_3 \rightarrow HO_2 + O_2 \quad (2)$$

$$ClO + HO_2 \rightarrow HOCl + O_2 \quad (3)$$

$$HOCl + h\nu \rightarrow OH + Cl \quad (4)$$

$$O_3 + O_3 \rightarrow 3O_2$$

Cycle II

$$Cl + O_3 \rightarrow ClO + O_2$$

$$Br + O_3 \rightarrow BrO + O_2 \quad (5)$$

$$BrO + ClO \rightarrow Br + Cl + O_2 \quad (6)$$

$$O_3 + O_3 \rightarrow 3O_2$$

Cycle III

$$2(Cl + O_3 \rightarrow ClO + O_2)$$

$$ClO + ClO + M \rightarrow Cl_2O_2 + M \quad (7)$$

$$Cl_2O_2 + h\nu \rightarrow Cl + ClOO \quad (8)$$

$$ClOO + M \rightarrow Cl + O_2 \quad (9)$$

$$O_3 + O_3 \rightarrow 3O_2$$

We note that regeneration of HO_2 in cycle I is assumed to occur through reaction of OH with O_3. The reaction of ClO with OH could, however, compete with (2) for the high ClO and low O_3 concentrations found within the Antarctic vortex. The enhanced level of ClO in the Antarctic environment can also produce detectable amounts of OClO, produced by the reaction

$$BrO + ClO \rightarrow Br + OClO \quad (6')$$

Observations of OClO provide indirect evidence for the abundance of BrO and ClO and thus for the efficiency of Cycle II [*Tung et al.*, 1986; *Rodriguez et al.*, 1986]. Subsequent observations of OClO during the NOZE campaigns have provided quantitative estimates for the above cycle [*S. Solomon et al.*, 1987, 1989].

The above catalytic cycles pose requirements on the abundances of ClO, HOCl, HO_2, BrO, and NO_2 if they are to account for the observed ozone reductions during Antarctic spring. Cycles I–III require ClO mixing ratios between 0.5 and 1 ppbv (a factor of 100 enhancement over concentrations predicted by models with standard gas phase chemistry), HOCl concentrations between 0.5 and 1 ppbv, HO_2 number densities of 10^7 cm^{-3}, BrO abundances of order 10–20 pptv, and very low concentrations of NO_2 to prevent sequestering of ClO in chlorine nitrate [*Solomon et al.*, 1986; *McElroy et al.*, 1986*a*; *Rodriguez et al.*, 1986]. All of the theories achieve high concentrations of ClO by introducing heterogeneous reactions which transform chlorine reservoirs such as HCl or $ClNO_3$ into active chlorine. The following reactions have been proposed in this context:

$$ClNO_3 + HCl\ (ice) \rightarrow Cl_2 + HNO_3\ (ice) \quad (10)$$

$$ClNO_3 + H_2O\ (ice) \rightarrow HOCl + HNO_3\ (ice) \quad (11)$$

$$N_2O_5 + HCl\ (ice) \rightarrow ClNO_2 + HNO_3\ (ice) \quad (12)$$

In the above, the HCl is assumed to be adsorbed into ice/liquid particles in the stratosphere [*Molina et al.*, 1987].

The equilibrium concentrations of the active chlorine species are determined by the balance between the formation rates given by (10) and (11) and the availability of NO_x to reform $ClNO_3$. Higher concentrations of active chlorine species can be maintained in a denitrified atmosphere. The following reaction has been suggested to suppress NO_x:

$$N_2O_5 + H_2O\ (ice) \rightarrow 2HNO_3\ (ice) \quad (13)$$

Laboratory studies of (10)–(13) have also established that the nitric acid produced remains in the solid phase. Additional HNO_3 can be sequestered in the solid phase by direct freezing of nitric acid into polar stratospheric clouds (PSCs) [*Toon et al.*, 1986; *McElroy et al.*, 1986*b*; *Crutzen and Arnold*, 1986]. These processes provide temporary denitrification of the atmosphere until gas phase HNO_3 is rereleased and NO_x is produced by subsequent photolysis. Permanent denitrification is possible if HNO_3 (ice) is removed by particle deposition.

Laboratory studies of heterogeneous reactions prior to 1987 had concentrated on liquid sulfuric acid solutions [*Baldwin and Golden*, 1979; *Martin et al.*, 1980; *Harker and Strauss*, 1981; *Friedl et al.*, 1986; *Rossi et al.*, 1987]. These results indicated that the probability of reaction per gas surface collision (reaction efficiency) for reactions (10), (11), and (13) were at most 10^{-3} on sulfuric acid surfaces, while the rates required by the chlorine-related hypotheses were a factor of 10 higher. Recent laboratory measurements, however, indicate that the rates of heterogeneous reactions are extremely sensitive to the water content of the sulfuric acid aerosol [*Tolbert et al.*, 1988*b*; *Worsnop et al.*, 1988]. The heterogeneous reaction efficiencies over ice are found to be much larger than values determined over sulfuric acid surfaces. In addition, laboratory studies showed that HCl diffuses rapidly into ice surfaces [*Molina et al.*, 1987]. Reactions (10)–(13) could then proceed very rapidly on the surfaces of PSCs, which are probably mostly ice or ice/nitric acid crystals [*Steele et al.*, 1983; *Toon et al.*, 1986].

Existing data for heterogeneous reaction rates are summarized in Table 1. The recent measurements indicate that heterogeneous chemistry could occur fast enough to achieve significant conversion of HCl to $ClNO_3$ and active chlorine under Antarctic winter conditions. As discussed below, the final partitioning of chlorine species after simultaneous occurrence of (10)–(13) in the stratosphere can be sensitive to the relative magnitude of their rates, as well as to the initial concentrations of NO_x, $ClNO_3$, and N_2O_5. Uncertainties still remain regarding the following issues.

1. Although the rate of (10) seems fairly independent of the HCl concentration in ice for large molar fractions (>0.01), this rate does seem to depend on HCl concentrations at lower molar fractions [*Molina et al.*, 1987; *Leu*, 1988*a*]. The molar fraction of HCl in the particles responsible for dehydration could be about 0.001, an order of magnitude smaller than typical molar fractions in the above experiments. A linear dependence of the rate of (10) on the molar fraction of HCl, for example, could then slow down the rate of this reaction. Determination of the time constant for processing of HCl is particularly important, since rapid sedimentation of large PSC particles could provide a potentially important dechlorination mechanism.

2. As discussed in the next section, the amount of processed HCl depends crucially on the supply of NO_x available during this processing. If reactions (11) and (13) occur at a fast rate concurrently with (10) and (12), the available supply of NO_x will be reduced, and the conversion of HCl to active chlorine will be less efficient (see Figure 3 and accompanying discussion in the next section). Most of the experiments to date have been carried out on pure ice or ice-HCl surfaces with molar fractions of HCl of order 1% or larger. *Tolbert et al.* [1987] reported that the efficiency of (11) is substantially reduced in water/nitric acid substrates where the H_2O/HNO_3 ratio is less than 4.5, a composition typical of type 1 PSC particles. Measurements at different molar fractions of HCl by *Leu* [1988*a*, *b*] suggest that reactions (11) and (13) may be slower on HCl-ice surface than on a pure ice surface. It is thus important to obtain experimental data for the above reactions on ice-HNO_3 crystals, and for different molar fractions of HCl.

3. Conversion of HCl by Heterogeneous Chemistry

Reactions (10)–(13) will run to completion when the supply of HCl, $ClNO_3$, or N_2O_5 is exhausted. Examination of the stoichiometry of reactions (10) and (12) by *Wofsy et al.* [1988] yielded simple relations between the concentrations of initial reactants and net products after completion of HCl

TABLE 1. Available Kinetic Data on Heterogeneous Reactions

Reaction	Reaction Efficiency, γ	HCl/H_2O (Mole Fraction in Ice)	Reference/Comments
$ClNO_3 + H_2O \rightarrow HOCl + HNO_3$	1.0×10^{-5}		Sulfuric acid liquid surface [*Baldwin and Golden*, 1979]
	3.2×10^{-4}		Sulfuric acid liquid surface [*Rossi et al.*, 1987]
	2.6×10^{-3}		Sticking coefficient on sulfuric acid solution of 65% by mass at −63°C [*Tolbert et al.*, 1988*b*]
	~0.02	0	Ice at ~200 K [*Molina et al.*, 1987]
	0.009 ± 0.002	0	Ice-HNO_3 (185–208 K); $H_2O/HNO_3 > 4.5$ [*Tolbert et al.*, 1987]
	0.06 ± 0.03	0	[*Leu*, 1988*a*]; Reaction occurs up to at least $HCl/H_2O = 0.002$
$ClNO_3 + HCl \rightarrow Cl_2 + HNO_3$	0.05	0.0035	*Molina et al.* [1987]
	0.1	0.01	
			Tolbert et al. [1987]; Reaction occurs; HOCl detected for low HCl concentration
	$0.27^{+0.73}_{-0.13}$	>0.02	*Leu* [1988*a*]
	0.1	~0.002	HOCl detected
	$\sim 3 \times 10^{-3}$	0.002	Sticking coefficient on sulfuric acid solution of 65% by mass at −63°C [*Tolbert et al.*, 1988*b*]
$N_2O_5 + H_2O \rightarrow 2\ HNO_3$	$\geq 3.8 \times 10^{-5}$		Sulfuric acid liquid surface [*Baldwin and Golden*, 1979]
	2.9×10^{-3} exp $(-883/T)$		Sulfuric acid liquid surface 214–263 K [*Harker and Strauss*, 1981]
	$>1 \times 10^{-3}$	0	Ice at 185 K; NO_2 evolved? [*Tolbert et al.*, 1988*a*]
	0.028		Ice at 195 K [*Leu*, 1988*b*]
	0.05–0.09		Measured on $NH_3/H_2SO_4/H_20$ aerosols, 274–293 K, at relative humidities between 1% and 76% [*Mozurkewich and Calvert*, 1988]
$N_2O_5 + HCl \rightarrow ClNO_2 + HNO_3$	$>3 \times 10^{-3}$	0.07–0.14	Ice at 185 K [*Tolbert et al.*, 1988*a*]
	0.05–0.07	0.015–0.04	*Leu* [1988*b*]

conversion. We note, however, that Wofsy et al.'s argument assumed (1) adequate supply of NO_2 is maintained (for example, by photolysis of N_2O_5) during the heterogeneous conversion of HCl and (2) the rates of reactions (11) and (13) are negligible in comparison with those of (10) and (12). However, photolysis of N_2O_5 may not be able to maintain the supply of NO_2 at the large solar zenith angles typical of the Antarctic stratosphere during winter. At the same time, the reaction efficiencies of (10) and (12) could be smaller than those of (11) and (13) for molar fractions of HCl less than 0.01. Therefore the partitioning of chlorine species after heterogeneous processing must be examined with a detailed photochemical model.

In this section we first review the stoichiometric relations derived from reactions (10) and (12). Detailed model simulations are then presented to show that the time constants required to complete the heterogeneous processing and achieve these stoichiometric relations are determined by the rate of supply of NO_x, and are thus sensitive to available solar illumination. Model results also show that adoption of fast rates for reactions (11) and (13) can decrease the amount of converted HCl and significantly modify the derived stoichiometry. We stress that the adopted PSC scenario is not intended to reproduce any specific period during the 1987 winter-spring, but was chosen to illustrate the behavior of chlorine species under representative PSC conditions. The results below can then be used as guidelines to examine the processing by PSCs in the Arctic.

3.1. *Stoichiometric Relations*

We estimate that the concentration of $ClNO_3$ is about one third of that of HCl prior to the onset of heterogeneous chemistry (see Figure 4). This $ClNO_3$ will quickly react with an equal amount of HCl through (10) when PSCs appear. The amount of converted HCl can be larger than the initial $ClNO_3$ concentration when reaction (10) is amplified by the following sequence of reactions.

Sequence I

$$N_2O_5 + h\nu \rightarrow NO_2 + NO_3 \quad (14)$$

$$NO_3 + h\nu \rightarrow NO_2 + O \quad (15)$$

$$2(ClO + NO_2 + M \rightarrow ClNO_3 + M) \quad (16)$$

$$ClNO_3 + HCl\ (ice) \rightarrow Cl_2 + HNO_3\ (ice) \quad (10')$$

$$Cl_2 + h\nu \rightarrow 2\ Cl \quad (17)$$

$$2(Cl + O_3 \rightarrow ClO + O_2) \quad (18)$$

where we assume fast diffusion of HCl into the ice, and evolution of Cl_2 from the ice into the gas phase. If the N_2O_5 photolysis rate is fast enough to provide an excess of NO_x during the heterogeneous processing, the net effect of this sequence is to convert HCl and N_2O_5 to $ClNO_3$ and HNO_3 (ice), with the stoichiometry given by

$$N_2O_5 + HCl + 3\ h\nu + 2O_3 \rightarrow ClNO_3 + HNO_3\ (ice) + O + 2O_2 \quad (19)$$

Any $ClNO_3$ and HCl remaining after completion of (19) when N_2O_5 is exhausted react through (10) to yield additional active chlorine. The relation (19) is similar to the one suggested by *Wofsy et al.* [1988].

A different situation holds when the N_2O_5 photolysis is slow. If the photolysis of N_2O_5 is not fast enough to maintain

TABLE 2. Processing of HCl by Heterogeneous Chemistry

	Condition	Final Products
A:	$[N_2O_5]_i > [HCl]_i$	N_2O_5, $ClNO_3$, HNO_3 (ice)
A/B:	$[N_2O_5]_i = [HCl]_i$	$ClNO_3$, HNO_3 (ice)
B:	$[HCl]_i > [N_2O_5]_i > 0.5 \times ([HCl]_i - [ClNO_3]_i)$	Cl, $ClNO_3$, HNO_3 (ice)
B/C:	$[N_2O_5]_i = 0.5 \times ([HCl]_i - [ClNO_3]_i)$	Cl, HNO_3 (ice)
C:	$[N_2O_5]_i < 0.5 \times ([HCl]_i - [ClNO_3]_i)$	Cl, HCl, HNO_3 (ice)

the formation of $ClNO_3$, much of the product of HCl processing will remain in the form of active chlorine. The net effect of sequence I will then be

Sequence I'

$$N_2O_5 + 2HCl + 4h\nu \quad (20)$$

In this case, twice as much HCl can be processed by the same amount of N_2O_5, producing active chlorine.

Consideration of (12) running to completion in the dark, followed by photolysis of $ClNO_2$ upon return of sunlight yields the sequence

Sequence II

$$N_2O_5 + HCl\ (ice) \rightarrow ClNO_2 + HNO_3\ (ice) \quad (12')$$

$$ClNO_2 + h\nu \rightarrow Cl + NO_2 \quad (21)$$

$$Cl + O_3 \rightarrow ClO + O_2 \quad (22)$$

$$ClO + NO_2 + M \rightarrow ClNO_3 + M \quad (16')$$

$$N_2O_5 + HCl + h\nu + O_3 \rightarrow ClNO_3 + HNO_3\ (ice) + O_2 \quad (23)$$

Since the processed NO_x is sequestered in $ClNO_2$, formation of $ClNO_3$ does not occur until return of the sun. If sequence II occurs continuously in the sunlight, the situation is similar to that of sequence I.

Table 2 lists the possibilities for the final partitioning of chlorine and nitrogen species deduced from consideration of the stoichiometry of sequences I and II and of the fate of the excess HCl, $ClNO_3$, or N_2O_5. The subscript i denotes concentrations prior to the onset of heterogeneous chemistry, assumed to happen in July. In condition A, HCl is depleted before N_2O_5. With ample supply of NO_2 from the remaining N_2O_5, $ClNO_3$ is the final chlorine product. Sequences I and II run their course for conditions B and C until N_2O_5 is depleted, and the remaining HCl and $ClNO_3$ then react through (10). The difference between B and C is that $[N_2O_5]_i$ is large enough to convert all HCl to Cl and $ClNO_3$ in B, while a significant portion of HCl remains unprocessed in C. *Wofsy et al.* [1988] suggested that the above conditions could reflect the changes in partitioning of chlorine species with increasing levels of chlorine. This scheme would then explain the sudden onset of the ozone hole in the mid-1970s and its subsequent interannual behavior, if the concentration of N_2O_5 is such that the transition from A to B would occur at chlorine levels typical of the mid-1970s. The proportion of active chlorine will increase dramatically after that period, resulting in accelerated decrease of O_3. This question is addressed in the companion paper [*Ko et al.*, this issue].

3.2. *Model Results*

Substantial heterogeneous conversion of HCl requires a source of NO_x. This NO_x could be produced by photolysis of N_2O_5 during the winter months, as assumed above. Alternatively, NO_x could be supplied by photolysis of HNO_3 in September, or possibly by transport of NO_x into the chemically perturbed region (CPR). In any case, the time constants for net conversion of HCl to ClO and $ClNO_3$ will depend on the rate at which NO_x is supplied by the above processes. Detailed modeling is needed to determine how these time constants and net products of heterogeneous processing are affected by the amount of solar illumination, or by the inclusion of (11) and (13).

We first consider the case where reactions (11) and (13) are neglected and assume that the adopted reaction efficiencies γ for (10) and (12) (see Table 3) are constant for all molar fractions of HCl in ice. The calculations also assume 0.5 ppmv of H_2O frozen in type 2 particles with a 5-μm radius (equivalent to an extinction coefficient of about 9×10^{-3} km^{-1} at this altitude; see appendix for discussion of heterogeneous chemistry parameterization).

Figures 1 and 2 show the calculated time development of key chlorine and nitrogen species at 18 km between July 16 and August 30, at the latitudes indicated. The initial value of N_2O_5 on July 16 in Figure 1 is 0.7 ppbv and is chosen to achieve complete conversion of HCl to active chlorine, with negligible remaining amounts of $ClNO_3$ and N_2O_5 for present-day inorganic chlorine content of 3 ppbv in the upper stratosphere. Figure 2 adopts N_2O_5 concentrations of 1.4 ppbv. Initial conditions for Figure 2 and their significance will be discussed in more detail in section 4. Our choice of initial $ClNO_3$ and HCl concentrations is shown in Figure 4.

In the case of Figure 1, initial conversion of HCl to active chlorine is achieved rapidly (1–2 days) through reaction (10)

TABLE 3. Adopted Reaction Efficiencies (γ) for Heterogeneous Chemistry

Reaction	γ
$ClNO_3 + HCl\ (ice) \rightarrow Cl_2 + HNO_3\ (ice)$	0.1*
$ClNO_3 + H_2O\ (ice) \rightarrow HOCl + HNO_3\ (ice)$	0.01† (case 3) 0.001† (case 4)
$N_2O_5 + HCl\ (ice) \rightarrow ClNO_2 + HNO_3\ (ice)$	3×10^{-3}*
$N_2O_5 + H_2O\ (ice) \rightarrow 2\ HNO_3\ (ice)$	1×10^{-3}†

*Value at a molar fraction of HCl $m_{HCl} = 0.01$. From July 15 to August 1, we adopt this value at all molar fractions. After August 1, we assume the value to be constant for $m_{HCl} \geq 0.01$, and proportional to m_{HCl} for $m_{HCl} < 0.01$.

†For $m_{HCl} \leq 0.01$; 0 for $m_{HCl} > 0.01$, after August 1. We assume the values to be zero during the rapid heterogeneous processing prior to this date.

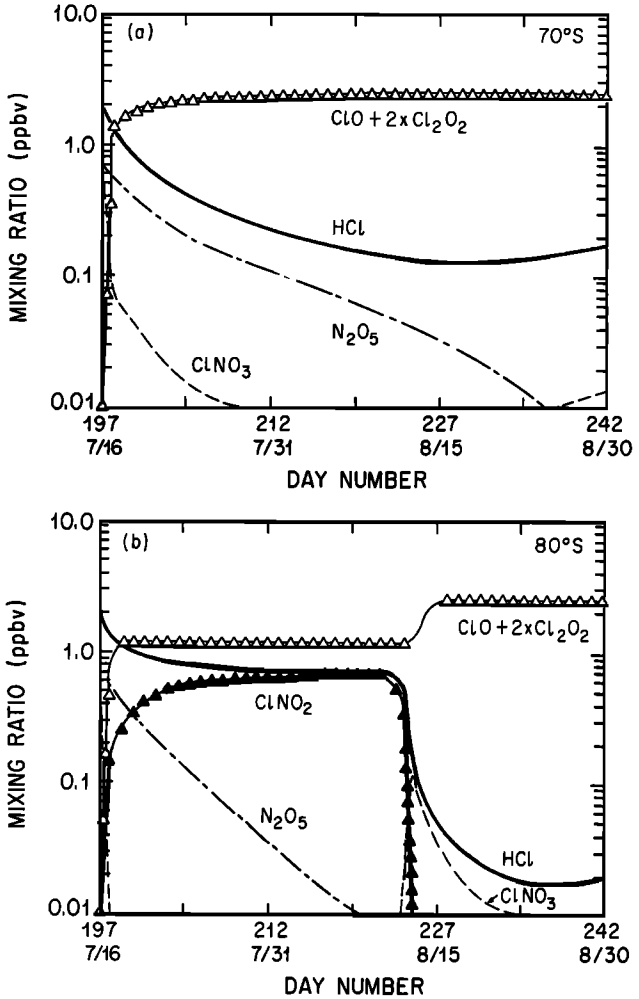

Fig. 1. Time development of chlorine and nitrogen species between July 16 (day 197) and August 30 (day 242) at 18 km with heterogeneous chemistry for (*a*) 70°S and (*b*) 80°S. An initial mixing ratio of 0.7 ppbv is adopted for N_2O_5. Reaction efficiencies for (11) and (13) are assumed to be zero. The PSC characteristics (see text) are not chosen to reproduce real-time conditions during 1987, but rather illustrate the behavior of trace species under heterogeneous chemistry. Initial concentrations of $ClNO_3$ disappear with a time constant of ~1 day through reaction (10). Curve labeled ClO + 2 × Cl_2O_2 also includes substantial concentrations of Cl_2 prior to emergence from polar night on day 224 at 80°S.

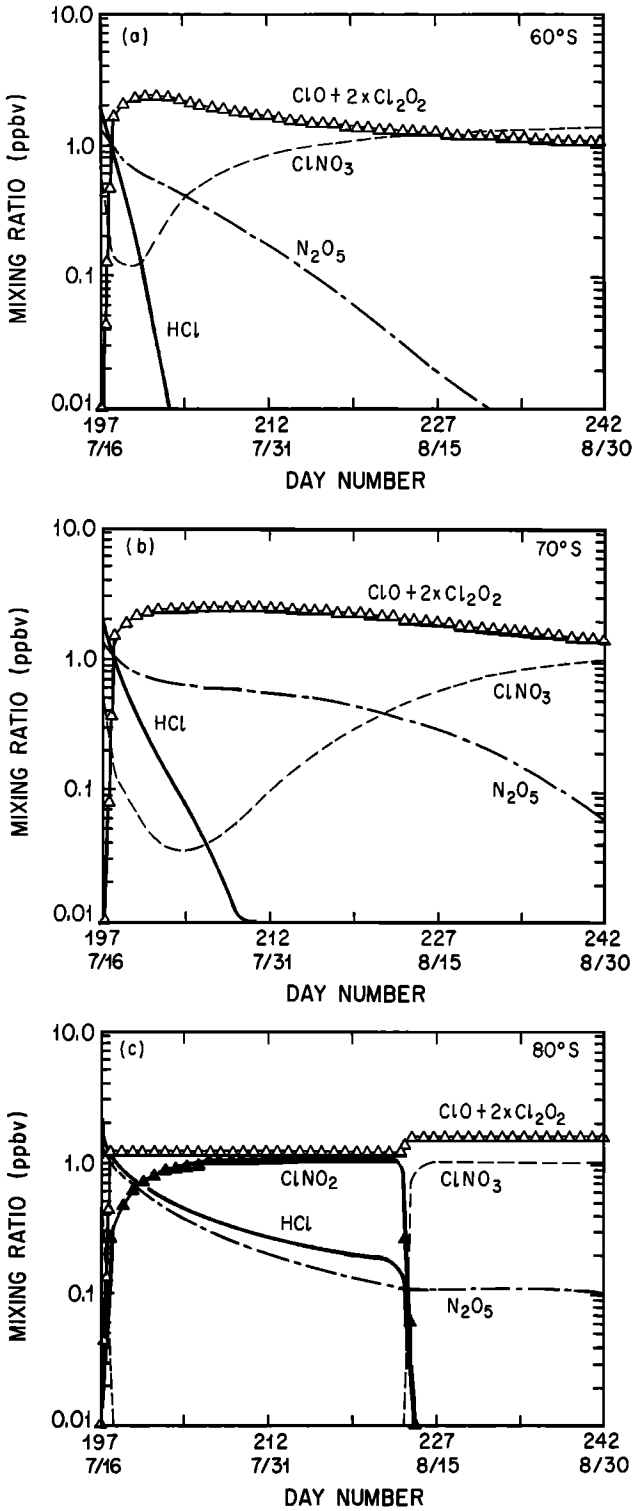

Fig. 2. Same as Figure 1, except for initial N_2O_5 mixing ratio of 1.4 ppbv. Results are shown for (*a*) 60°S, (*b*) 70°S, and (*c*) 80°S.

with the initial $ClNO_3$. For illuminations typical of 70°S (Figure 1*a*), this is followed by slower decrease/increase in HCl/active chlorine through sequences I and II. At 80°S (Figure 1*b*) the conversion occurs in two stages: through reaction (12) during polar night with a time constant of about 10 days, and through (10) after the return of the sun in mid-August with a time constant of 2–3 days. Although the final concentrations of HCl, $ClNO_3$, and active chlorine are those predicted by the stoichiometric relations discussed above, the time required to reach these values can be as long as 1 month. A large fraction of the HCl remains in the gas phase until the return of sunlight for 80°S conditions.

The larger initial concentrations of N_2O_5 adopted in Figure 2 result in faster conversion of HCl at 60°S and 70°S (Figures 2*a* and 2*b*) through sequence I. Substantial concentrations of $ClNO_3$ are produced as N_2O_5 photolyzes and $ClNO_3$ is formed. Concentrations of N_2O_5 and $ClNO_3$ decrease/increase with a time constant of 20–30 days at 70°S. At 80°S the mechanism is similar to Figure 1. Final concentrations of chlorine species are again similar to those predicted by the stoichiometry.

The above stoichiometry and calculations assume that (11) and (13) are negligible. If N_2O_5 or $ClNO_3$ are removed rapidly by heterogeneous reactions (11) and (13) during

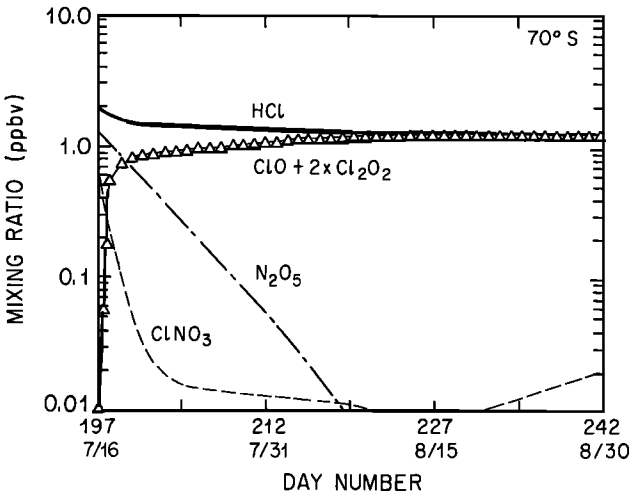

Fig. 3. Same as Figure 2*b*, except that reaction efficiencies for (11) and (13) are taken as 5×10^{-3} and 1×10^{-2}, respectively.

August, the final partitioning of chlorine species could be different. This situation is illustrated in Figure 3, where we have assumed reaction efficiencies of 1×10^{-2} and 5×10^{-3} for reactions (11) and (13), respectively. N_2O_5 and $ClNO_3$ are then removed rapidly through (11) and (13). As a result, a large fraction of the HCl remains unprocessed.

The unprocessed HCl in Figure 1*b* or Figure 3 could be incorporated into large sedimenting ice particles, leading to substantial dechlorination of the lower stratosphere. Estimates of the total chlorine budget by *Gandrud et al.* [1988] indicate that some of the air sampled during the AAOE mission may indeed have been dechlorinated. Reactions (11) and (13) could thus be important in modulating possible nonlinearities in the partitioning of chlorine species in different years (see also *Turco et al.* [this issue]). It is thus important to clarify the effect of reactions (11) and (13) by further kinetic data and by measurements of the concentrations of chlorine and nitrogen species during austral winter months.

Heterogeneous chemistry could continue to play an important role after the initial processing described in the above calculations. Reaction (11) can reduce the initial amounts of $ClNO_3$, while reaction (10) can retard the formation of HCl during September. The role of these reactions during the AAOE period can be ascertained by comparison of calculations and observations. The calculations presented below will address this question.

4. Approach and Assumptions

Most of the mechanisms driving the photochemistry in the spring Antarctic environment need sunlight. The low levels of illumination at the season, latitude, and altitudes of interest imply that the time constants for important mechanisms (HNO_3 photolysis, reformation of HCl) are of order 10–30 days. Complete modeling of the Antarctic stratosphere would then require consideration of the illumination conditions for an ensemble of air parcels representative of different latitudes, altitudes, and time periods.

Examination of the photochemistry along air parcel trajectories derived from meteorological data [*Jones et al.*, 1989; *Austin et al.*, this issue] addresses some of these issues. This approach is appropriate for the detailed analysis of in situ measurements of species with time constants of less than 10 days. Uncertainties in the initial conditions and in the precise parcel trajectories, however, make this approach unsuitable in the study of the behavior of Antarctic species with longer time scales, such as O_3. Consideration of the specific details in the history of a particular air parcel also makes it harder to study the sensitivity of large-scale behavior of trace gases to uncertainties in kinetic data and initial conditions.

Our study stresses the behavior of different species inside the vortex on both large spatial and long temporal scales. We illustrate the effects of different illumination levels by carrying out diurnal calculations for air masses at fixed latitudes of 60°, 70°, and 80°S. These calculations are time-stepped forward from July 15 to the end of October. The long-lived species in our simulations are initialized by taking into account the constraints placed by AAOE data. This initialization thus includes the effects of transport on the long-lived trace gases. Results of the different simulations are then evaluated by comparison with relevant observations of short-lived trace gases by the different AAOE instruments located onboard either the NASA ER-2 high-altitude aircraft or the NASA DC-8 medium-altitude aircraft. Such evaluation sheds light on possible constraints placed by AAOE observations, particularly on initial concentrations of nitrogen oxides, and spatial extent and duration of heterogeneous mechanisms. Simulations are then used to extrapolate the behavior of different species to periods not covered by the AAOE campaign. This approach is best suited to address the questions discussed in the introduction and complements the short time scale analysis of air parcel studies.

We present results for four different cases, whose assumptions are summarized in Table 4. These cases were chosen specifically to study the sensitivity of the Antarctic chemistry to initial concentrations of nitrogen oxides prior to the

TABLE 4. Cases Considered

Case	Initial N_2O_5 (July 15)*	Heterogeneous Chemistry
1	$0.5 \times ([HCl]_i - [ClNO_3]_i)$	until August 1
2	$0.67 \times [HCl]_i$†	until August 1
3	$0.67 \times [HCl]_i$†	until mid-September (see text)
4	$0.67 \times [HCl]_i$†	until mid-October (see text)

*Subscript *i* denotes species concentration prior to onset of heterogeneous chemistry on July 15.
†Value chosen to simulate onset of active chlorine production by heterogeneous chemistry during mid-1970s (see text).

onset of heterogeneous chemistry and the magnitude and duration of heterogeneous reactions. In particular, our choice of cases assesses the role of the nonlinearity discussed by *Wofsy et al.* [1988] (see also section 3) in controlling the decadal behavior of O_3 [*Ko et al.*, this issue]. Further details on our choice of cases are discussed below. The results of the cases presented bracket a number of observations from the AAOE experiments, after allowing for uncertainties in the actual illumination of the air parcels and the spread in the data.

The calculations adopt the latest recommendations for gas phase reactions [*NASA Panel for Data Evaluation*, 1987]. Photolysis rates are calculated using a multiple-scattering code that takes into account the sphericity of the atmosphere in the absorption of radiation. Formation rates of Cl_2O_2 are taken from *Hayman et al.* [1986]. Photolysis rates of Cl_2O_2 are calculated from the absorption cross sections of *Molina and Molina* [1987] (see discussion in Appendix B). Rates and branching for the reaction of BrO with ClO are those of *Sander and Friedl* [1988]. Background densities and temperatures are taken from an average of the meteorological measurement system (MMS) measurements aboard the ER-2 within the vortex, for altitudes between 12 and 18 km [*Chan et al.*, 1989]. These averages were within 10% of those calculated from the balloon measurements of temperature and pressure at McMurdo during 1986 [*Hofmann et al.*, 1987]. We therefore used the balloon results to extend our model atmosphere to higher and lower altitudes.

The model simulation is divided into two regions: 12–22 km and 22–50 km. The chemistry in the region between 22 and 50 km is assumed to be the same for all cases considered. Calculations are initialized from the results of the Atmospheric and Environmental Research, Inc. (AER) two-dimensional model [*Ko et al.*, 1985]. Ozone between 22 and 30 km is initialized with the values of *Hofmann et al.* [1987] and joined smoothly to the results of the two-dimensional model above 30 km. Ozone concentrations below 22 km are updated daily from the calculated photochemical production and loss. We discuss below our assumptions regarding the following: (1) initial conditions for long-lived species, (2) denitrification processes and concentrations of nitrogen species, (3) temporal and spatial behavior of heterogeneous chemistry, and (4) choice and interpretation of observational constraints for our calculations.

4.1. *Initial Conditions for Long-Lived Species*

We utilize measurements of long-lived species from the AAOE campaign to constrain initial conditions for our model below 18 km. Profiles between 18 and 22 km, where no in situ ER-2 observations are available, are obtained by scaling results from the AER two-dimensional model to observations below 18 km, except as noted below. Calculations are initialized on July 16 as follows.

1. ClY ($Cl + 2 \times Cl_2 + 2 \times Cl_2O_2 + ClO + ClNO_3 + ClNO_2 + OClO + HCl$) abundances are derived from the average of organic chlorine measurements by the whole-air sampler on the ER-2 [*Heidt et al.*, 1989] and closure considerations. The HCl and $ClNO_3$ profiles in Figure 4 are taken as initial conditions on July 15, prior to the onset of heterogeneous chemistry. The partitioning for these species at high latitudes during winter has been calculated in a manner similar to that described by *McElroy et al.* [1986*a*].

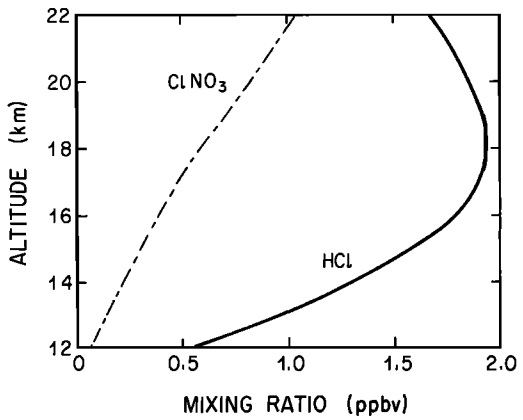

Fig. 4. Initial concentrations of HCl and $ClNO_3$ adopted on July 16.

2. CH_4 is taken from the whole-air sampler measurements inside the vortex [*Heidt et al.*, 1989].

3. Water mixing ratios are taken to be 3 ppmv between 12 and 22 km [*Kelly et al.*, 1989].

4. Initial ozone concentrations below 18 km are taken from the ER-2 measurements on August 23 [*Proffitt et al.*, this issue; *Starr and Vedder*, 1989]. Values above and below this altitude are taken from the August balloon measurements of *Hofmann et al.* [1987] from McMurdo.

4.2. *Denitrification and Concentrations of Nitrogen Species*

Model results will also depend on the initial concentration and partitioning of NO_y species. Analysis of the measurements by the NO_y detector onboard the ER-2 [*Fahey et al.*, this issue] indicate gas phase mixing ratios of NO_y of 10 ± 2 ppbv near 60°S outside the ClO wall defining the vortex, 3 ± 1 ppbv near 70°S just inside the vortex, and values less than 2 ppbv at locations deeper into the vortex. The measured NO_y exhibits no noticeable altitude gradient. The NO_y concentrations in our calculations must satisfy these observational constraints during the AAOE period inside the vortex, both in the "collar" region near the edge and in the "core" region toward the center.

The NO_y observations indicate that nitrogen species have been removed from the gas phase inside the vortex. Denitrification in the lower stratosphere could occur in two different ways: (1) nitric acid could be frozen directly into PSC particles at the phase transition temperature [*Toon et al.*, 1986; *McElroy et al.*, 1986*b*; *Crutzen and Arnold*, 1986], and (2) nitrogen oxides in N_2O_5 and $ClNO_3$ could be changed to solid HNO_3 through the heterogeneous reactions (10)–(13).

Modeling of the detailed microphysics of PSC formation and evolution is beyond the scope of this paper [e.g., *Toon et al.*, 1989; *Turco et al.*, this issue; *Poole and McCormick*, 1988]. We assume instead that direct freezing of HNO_3 occurs by July 15. Our choice of gaseous HNO_3 mixing ratios on July 15 has been guided by three criteria: (1) the concentrations calculated by the AER two-dimensional model serve as upper bounds, (2) the in situ NO_y concentrations measured aboard the ER-2 within the vortex constrain the total amount of nitrogen calculated in the model,

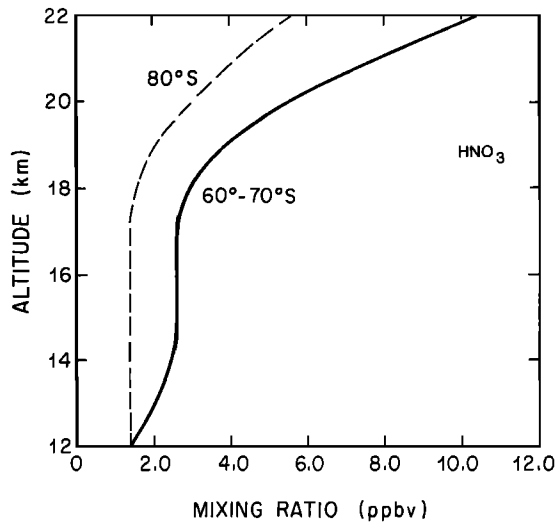

Fig. 5. Mixing ratios of HNO_3 adopted on July 16.

and (3) the calculated HNO_3 throughout the measuring period should be consistent with the total column measurements from the infrared instrument on the DC-8. The adopted HNO_3 profiles for the four cases at different latitudes on July 15 are shown in Figure 5. Since the measured column density of HNO_3 decreases toward the center of the vortex, the nitric acid profile for the 80° run has been reduced accordingly. The profile in Figure 5 represents a 60–80% reduction in the nitric acid abundances calculated by the AER two-dimensional model. We must stress, however, that the adopted HNO_3 and NO_y profiles do not represent a unique way to satisfy the constraints placed by measurements.

The adopted initial concentration of nitric acid on July 15 is interpreted as a saturation mixing ratio of gaseous HNO_3 over PSCs. We then assume that these abundances are upper bounds for nitric acid in the gas phase during the period of the calculations (July–October). Nitric acid produced by reactions (10)–(13) is initially released in the gas phase but is immediately incorporated into the solid phase if the gaseous HNO_3 mixing ratios are equal to or larger than the adopted saturation values. Our calculations allow for loss of nitric acid through photolysis or reaction with OH. Possible release of nitric acid through particle evaporation has not been included.

The discussion in section 3 pointed out the importance of odd nitrogen ($NO_x + 2 \times N_2O_5 + ClNO_3$) abundances prior to the onset of heterogeneous chemistry (Table 2). The initial concentrations of N_2O_5 are uncertain, given the possibility of reaction (13) occurring on background aerosols [*Harker and Strauss*, 1981; *Austin et al.*, 1986; *Worsnop et al.*, 1988; *Mozurkewich and Calvert*, 1988]. Since there are no data on N_2O_5 concentrations during July, we have considered cases reflecting different initial levels of N_2O_5 and thus different efficiency for converting HCl to active chlorine.

Our choice of N_2O_5 for case 1 yields complete conversion of HCl, $ClNO_3$, and N_2O_5 to active chlorine and HNO_3 for present-day conditions during July (see Figure 1), thus placing the transition B/C (Table 2) at current levels of chlorine. This case represents the maximum levels of active chlorine available for present-day conditions. Reactions (10)–(13) are then negligible until HCl and $ClNO_3$ are reformed in mid-September. The initial conditions for N_2O_5 in cases 2–4 place the transition A/B in Table 2 during the late 1970s, at a chlorine level of 2.0 ppbv. The adopted N_2O_5 concentrations are thus equal to the HCl abundances for this level of chlorine. Production of both $ClNO_3$ and active chlorine then occurs during July–August for present-day conditions (see Figure 2).

4.3. *Temporal and Spatial Behavior of Heterogeneous Reactions*

Polar stratospheric clouds are observed to appear during June–July, starting first at high altitudes and moving to lower altitudes, finally disappearing sometime during September–October. Although the spatial and temporal behavior of PSCs described below is not intended to reproduce conditions during 1987, our choices have incorporated general features of the observed behavior of PSCs. We treat heterogeneous chemistry as follows.

1. All heterogeneous reactions are parameterized in terms of collision frequency of gas molecules with reacting surfaces, and probability of reaction per collision. Details of the parameterization of heterogeneous reactions are discussed in Appendix A.

2. We assume for simplicity two stages for the heterogeneous chemistry.

During the first stage (July 16 to August 1 for 60°S and 70°S calculations, July 16 to August 15 for 80°S calculations), HCl is converted to active chlorine and chlorine nitrate by (10) and (12) as discussed in section 3. We maximize heterogeneous conversion of HCl by neglecting reactions (11) and (13) during this period of time. Heterogeneous chemistry is assumed to occur on ice particles (type 2) with a radius of 5 μm, formed by freezing 0.5 ppmv of H_2O at all altitudes. These particles may subsequently sediment, thus yielding a dehydrated stratosphere during AAOE [*Kelly et al.*, 1989]. We note that the abundances of trace species at the end of this stage for 18 km are the same as those shown in Figures 1 and 2 on August 1 (60°S and 70°S calculations) and August 15 (80°S calculations).

The second stage extends from August 1 (60° and 70°S) and 15 (80°S) until the end of October. Heterogeneous chemistry during this period converts residual $ClNO_3$ and/or N_2O_5 to active chlorine and/or $ClNO_3$ through reactions (11) and (13). Reformation of HCl can be retarded by reaction (10). We consider three possibilities, bracketing the latitudinal and temporal extent of heterogeneous activity.

The first possibility, no heterogeneous activity (cases 1 and 2), addresses the question of whether heterogeneous chemistry is needed during the AAOE period. Reaction efficiencies of (10)–(13) on PSC surfaces could be much smaller than those measured on ice surfaces in the laboratory if, for example, large HNO_3/H_2O concentrations in the ice substantially affect the heterogeneous kinetics [*Tolbert et al.*, 1987].

For the second possibility, moderate PSC extent and duration (case 3), we adopt a gas-aerosol collision frequency corresponding to an average extinction coefficient for PSCs of 2×10^{-3} km^{-1} for the 60° and 70° cases on August 1, and of 3×10^{-3} km^{-1} for the 80° case on August 15, at all altitudes between 12 and 22 km. We assume a particle radius of 1 μm during this period, with an average molecular weight representative of a nitric acid trihydrate crystal. The extinc-

tion coefficients decrease linearly throughout the period to a zero value on days between September 1 (high altitude end) and September 15 (low altitudes), for the 60° and 70° cases. In the 80° calculations, complete disappearance of PSCs is assumed to occur between September 15 (high altitudes) and October 1 (low altitudes). This case could be interpreted as representing typical "thin haze" conditions for PSCs.

For the third possibility, long-lived PSCs (case 4), we choose a collision frequency corresponding to an extinction coefficient of 2×10^{-3} km^{-1} at 18 km for all latitudes. The altitude profile of the extinction coefficient is scaled with the adopted partial pressure of HNO_3. We assume that these extinction coefficients are constant until October 15. Heterogeneous processing can thus occur until this date for this scenario. These conditions are suggestive of the behavior during 1987, when PSCs were observed into October by the SAM II instrument (M. P. McCormick, private communication, 1988).

Adopted reaction efficiencies for (10)–(13) are listed in Table 3. We have simulated the possible decrease of the rate of (11) on nitric acid trihydrate crystals [*Tolbert et al.*, 1987] by reducing this rate by a factor of 10 in case 4, thus maintaining high concentrations of $ClNO_3$ during the AAOE measurement period.

4.4. *Observational Constraints*

The following sets of measurements were used to evaluate the results of the different cases: ClO measurements aboard the ER-2 [*Brune et al.*, this issue] and column densities of HNO_3, HCl, $ClNO_3$, and NO_2 aboard the DC-8 [*Toon et al.*, this issue; *Coffey et al.*, this issue; *Mankin and Coffey*, 1989].

Comparison of our results to local and column O_3 densities are discussed by *Ko et al.* [this issue]. We do not use the NO column densities measured by the infrared spectrometers aboard the DC-8, since most of the contribution to this column comes from altitudes above 22 km, outside our region of interest. Our calculated NO mixing ratios in early September for all cases are less than 10 pptv inside the vortex. Since these values are much smaller than the observation threshold of 30 pptv for the NO_y detector [*Fahey et al.*, this issue], these measurements cannot help in discriminating among the different simulations. Analysis of OClO column measurements at twilight has not been completed at this time. We thus do not include results on OClO in this paper.

Care must be taken in comparing model results with observations for species whose characteristic time constants are larger than a few days. In these cases, the measured concentrations will reflect the history of the sampled air parcel. For example, comparison of ER-2 observations near 70° with model results at this latitude must take into consideration the behavior for the 60° and 80° curves. Such an approach can then indicate whether apparent discrepancies can be used to rule out specific cases, or whether they could be a result of latitude excursions.

5. RESULTS

We present below results of our calculations for cases 1–4 and compare them with pertinent measurements from the AAOE mission. Our simulations have indicated that calculated HCl and ClO are particularly sensitive to assumptions about initial conditions and duration of heterogeneous chemistry. We therefore stress the comparison with measurements of these species.

Column density measurements from the NCAR and JPL infrared spectrometers onboard the DC-8 have been sorted into bins centered around 70° and 80°S and averaged for each day of measurements. The bars around the data points shown in the figures extend from the minimum to the maximum value in each bin. We have averaged together results from both instruments for HNO_3, NO_2, and $ClNO_3$, since there is good agreement between both sets of measurements. There exists a discrepancy between the NCAR and JPL measurements of HCl [*Toon et al.*, this issue; *Coffey et al.*, this issue]. Comparison for this species treats both sets separately.

5.1. *HNO_3*

Measured column densities of HNO_3 decrease from about $1.3–1.6 \times 10^{16}$ cm^{-2} in the "collar" region to $0.5–0.8 \times 10^{16}$ cm^{-2} in the "core" region of the vortex. Our calculated column densities of HNO_3 for cases 1 and 4 are shown in Figure 6, compared with the data from the JPL and NCAR infrared spectrometer instrument aboard the DC-8. Results for the other cases are very similar to case 1 and thus not shown. The contribution to the total column density from altitudes above 22 km is about 30% for 60° and 70° conditions, and 50% for the 80° case. Since our choice of initial profiles for HNO_3 was guided by the in situ NO_y measurements, our results suggest a general consistency between the total HNO_3 column measurements and the observations of NO_y.

Case 1 assumes no heterogeneous processing during September. The decrease in the nitric acid column density in Figure 6*a* is due to photolysis of HNO_3 and reaction with OH. Calculated column densities of HNO_3 in case 4 (Figure 6*b*) decrease less rapidly. This is because photodecomposition of HNO_3 is compensated by production of nitric acid by heterogeneous chemistry when gas phase HNO_3 abundances fall below the assumed saturation value.

5.2. *NO_2*

Vertical column densities of NO_2 calculated for case 1 in the afternoon twilight are compared in Figure 7 with the average of measurements by the JPL and NCAR infrared spectrometer. Results for other cases behave similarly. The absolute value of the observed column densities are about a factor of 2 lower than calculations, particularly for the core region near 80°S. We note that 90% of the column density of NO_2 on September 15 lies above 22 km.

Our calculations adopt the results of the AER two-dimensional model above 22 km, which are consistent with the measurements outside the vortex. *McCormick and Larsen* [1986] have pointed out that the NO_2 densities observed by the SAGE and SAM II instruments inside the vortex are about a factor of 2 lower than those outside up to 40 km. The discrepancy between calculations and observations is thus not a symptom of the chemical scheme adopted for the low-altitude region, but rather of the adopted NO_2 and/or NO_y at higher altitudes.

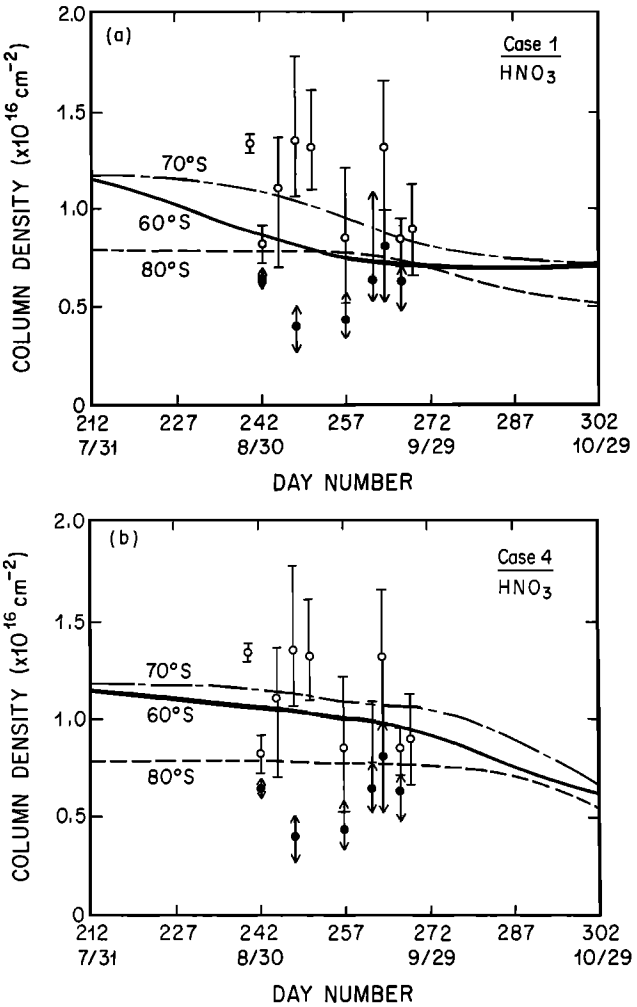

Fig. 6. Calculated HNO_3 column densities for 60° (solid line), 70° (dash-dot line), and 80°S (dashed line) conditions, for (*a*) case 1 and (*b*) case 4 compared with average of data from the JPL and NCAR infrared spectrometers, binned around (open circles) 70°S and 80°S (solid circles).

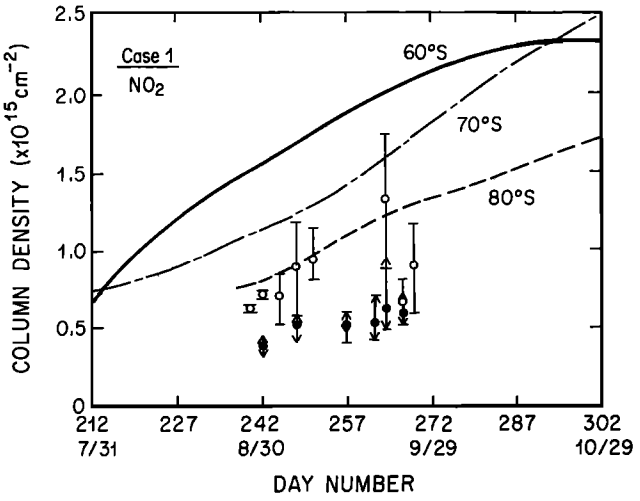

Fig. 7. Calculated NO_2 column densities in the afternoon twilight for case 1, compared with average of results from the JPL and NCAR infrared spectrometers near 70°S (open circles) and 80°S (solid circles). Calculations for different latitudes are denoted as in Figure 6.

5.3. *$ClNO_3$*

Measured $ClNO_3$ column densities decrease from values between 2 and 4 × 10^{15} cm^{-2} in the collar region to values near 1 × 10^{15} cm^{-2} in the core of the vortex. Calculated column densities of $ClNO_3$ are compared with the average of observations by the JPL and NCAR spectrometers in Figures 8*a* (case 1), 8*b* (case 2), 8*c* (case 3), and 8*d* (case 4).

Calculations at 60° and 70° for case 1 (Figure 8*a*) are consistent with the lower bound of observations in this latitude bin after September 15. Column densities observed near 80°S, although higher than the case 1 results at this latitude, lie in the area bounded by the 70° and 80° curves. Allowing for uncertainties in the illumination history of the sampled air masses and in the calculated column density of $ClNO_3$ above 22 km, the results of case 1 imply that photolysis of nitric acid could supply enough NO_x to account for $ClNO_3$ column densities of up to 2 × 10^{15} cm^{-2} after mid-September. It is, however, difficult to explain the very high column densities of $ClNO_3$ measured on four different days (September 5, 8, 19, and 26).

Column densities of $ClNO_3$ as high as 3 × 10^{15} cm^{-2} can be obtained in early September if we assume excess initial N_2O_5 and a negligible rate for (11) (case 2). High column densities of chlorine nitrate could also be obtained in early September if fresh NO_x were supplied from outside the vortex by mixing processes. Comparison of results of case 2 with observations in Figure 8*b* suggest that this condition could explain the very high $ClNO_3$ column densities in the collar region near 70°S. However, the large column densities of chlorine nitrate predicted by this case are not observed in the inner core region.

The adoption of a fast rate for (11) in case 3 after August 1 leads to rapid conversion of $ClNO_3$ to HOCl and active chlorine. The results for case 3 (Figure 8*c*) are thus very similar to those of case 1 after the beginning of September. The slower rate for (11) adopted in case 4 (Figure 8*d*) leads to slower conversion of $ClNO_3$ to active chlorine. Results of both cases 3 and 4 are again consistent with observations, if we exclude the high values discussed above.

5.4. *HCl*

Calculated column densities of HCl are shown in Figures 9*a* and 9*b* (case 1 compared with JPL and NCAR data, respectively) and 9*c* and 9*d* (case 4 compared with JPL and NCAR data, respectively). Results for cases 2 and 3 are similar to those of case 1.

Calculations in early September are generally consistent with the JPL measurements shown in Figure 9*a* but are larger than the NCAR values (Figure 9*b*). The low values observed for the HCl column densities require almost complete removal of HCl between 12 and 22 km. We have achieved this in our model by conversion of HCl to other forms of chlorine by reactions (10) and (12) during July on type 2 PSCs. The HCl could also be processed with longer time constants on type 1 (nitric acid trihydrate) PSCs. Heterogeneous processing could start with the appearance of type 1 PSCs in June and be essentially complete by the time of the appearance of type 2 aerosols in late July [*Poole and McCormick*, 1988; *Toon et al.*, 1989; *Turco et al.*, this issue].

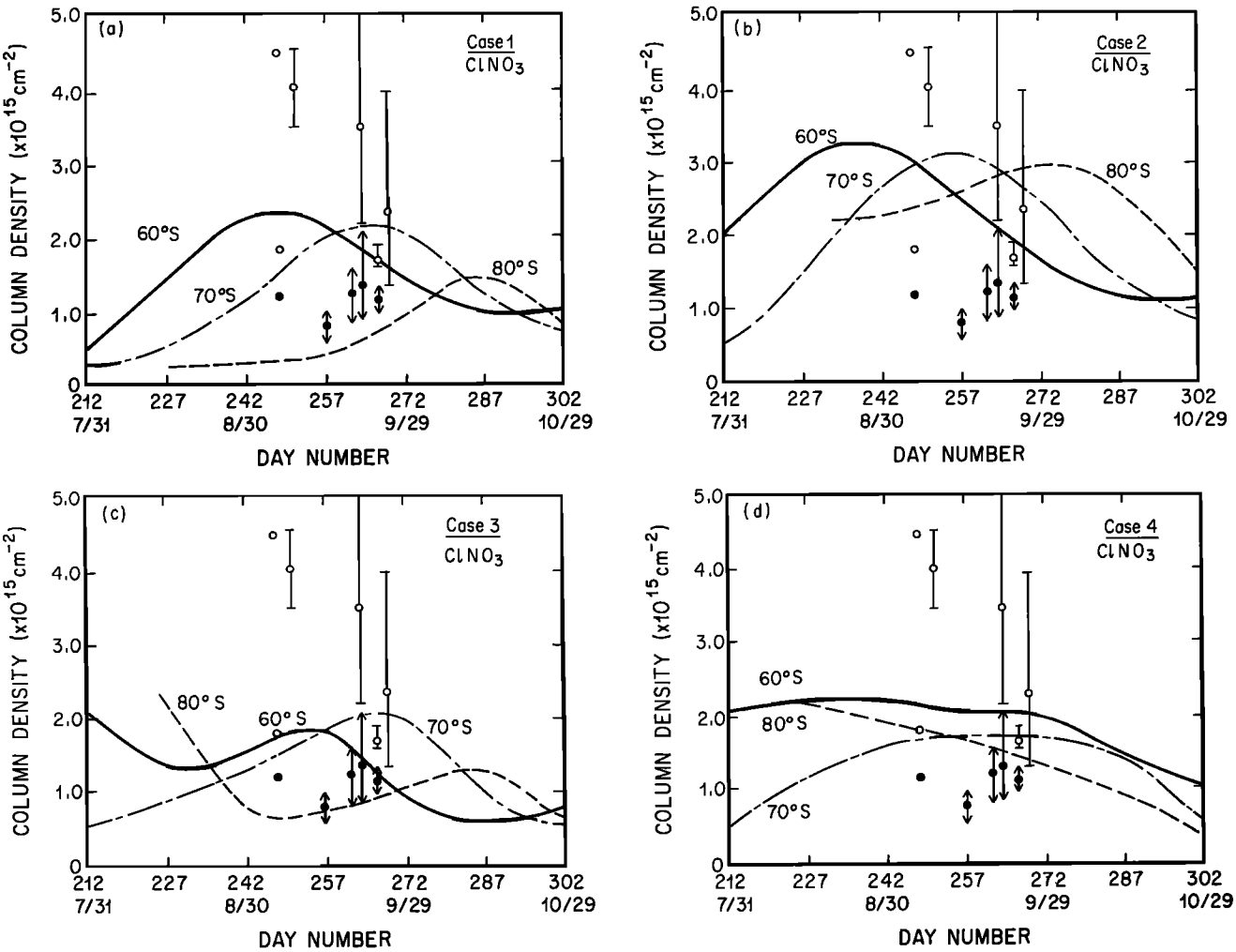

Fig. 8. Calculated column densities of chlorine nitrate at noon for cases (*a*) 1, (*b*) 2, (*c*) 3, and (*d*) 4 compared with average of data from the JPL and NCAR infrared spectrometers near 70°S (open circles) and 80°S (solid circles). Calculations for different latitudes are denoted as in Figure 6.

If the rates for (11) and (13) are faster than for (10) and (12) on PSCs, abundances of NO_x and $ClNO_3$ could be much smaller in winter. In this case, about one half of the HCl could remain unprocessed during the month of August (see Figure 3), resulting in column densities of order 3–4 × 10^{15} cm^{-2}. Calculations (not shown) indicate that photolysis of HNO_3 during September does not produce sufficient NO_x to process the above HCl. Recent measurements of the solubility of HCl [*Hanson and Mauersberger*, 1988] make it unlikely that this amount of HCl could be frozen in type 1 PSCs. The unprocessed HCl could, however, be dissolved in large sedimenting type 2 (ice) particles, resulting in its permanent removal from the Antarctic lower stratosphere [*Turco et al.*, this issue; *Gandrud et al.*, 1988]. This dechlorination scenario yields low column densities of HCl, while enough active chlorine is produced to give results consistent with ClO observations (see Figure 3). Therefore dechlorination is not ruled out by the AAOE data. Resolution of this issue requires further laboratory data on the rates of (10)–(13) for different concentrations of HCl and HNO_3, as well as measurements of HCl and NO_x during winter, and on the solubility of HCl in PSCs.

Reformation of HCl through the reaction

$$Cl + CH_4 \rightarrow HCl + CH_3 \quad (24)$$

starts in early September at 60° and 70°S, and in the second half of September at 80°S, in the absence of heterogeneous chemistry (case 1). The calculated recovery of HCl for this case is faster than observed, particularly at 70°S. Adoption of fast heterogeneous processing in case 4 retards the calculated recovery, thus giving better agreement with observations (Figures 9*c* and 9*d*).

5.5. *ClO*

Calculated concentrations of ClO are compared with measurements aboard the ER-2 near 70°S [*Brune et al.*, this issue] in Figure 10 (14 km, 396 K potential temperature), Figure 11 (16 km, 404 K potential temperature), and Figure 12 (18 km, 444 K potential temperature). For each figure, panels *a*, *b*, *c*, and *d* correspond to cases 1, 2, 3, and 4, respectively. The data displayed are taken from the southernmost segment of the flights, where the ER-2 executes a dive to lower altitudes. This segment usually occurs in the deepest incursion of the aircraft into the vortex. Concentrations of ClO in the core region deep inside the vortex are not

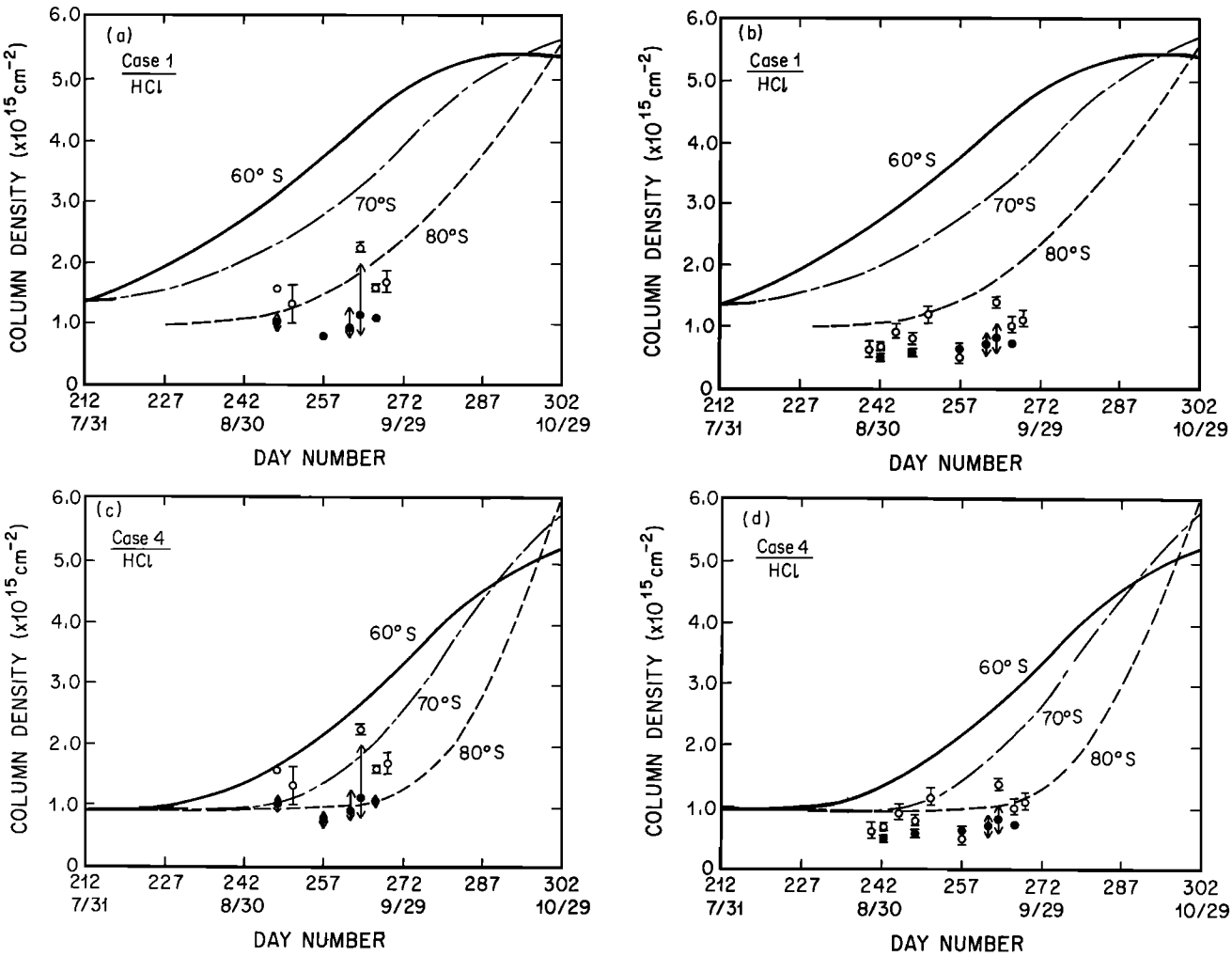

Fig. 9. Calculated column densities for HCl at noon for (*a*, *b*) case 1 and (*c*, *d*) case 4, compared with data from the (*a*, *c*) JPL and (*b*, *d*) NCAR infrared spectrometers. Data near 70°S and 80°S are indicated by open and solid circles, respectively. Calculations for different latitudes are denoted as in Figure 6.

available from the ER-2 data, although values around 1.5 ppbv have been obtained by ground-based observations at McMurdo during NOZE II [*de Zafra et al.*, 1989].

Results for cases 1–4 bracket the observations. Calculated concentrations for case 2 are in general lower than most measurements, particularly at the highest altitude. Model results suggest that the observed ClO thus seems too high to be compatible with the high column densities of $ClNO_3$ measured in the collar region. We note, however, that changes in the kinetic data for Cl_2O_2 could change the partitioning of chlorine species and allow for the coexistence of high densities of ClO and $ClNO_3$ (see Appendix B). Better agreement is obtained at the highest altitude between the results of cases 1, 3, and 4 and observations during early September. The calculated abundances of ClO for these cases are, however, higher than observations by 30–50% at the lower altitudes. This could be an indication of less efficient conversion of HCl to active chlorine than assumed by our calculations at these altitudes.

The high mixing ratios of ClO observed in early September are maintained at all altitudes until the last ER-2 flight (September 22). Calculations at 60° and 70° for cases 1 and 2 exhibit a rapid decrease in ClO starting in the early half of September. This decrease is due to conversion of active chlorine to $ClNO_3$ and HCl in the absence of heterogeneous chemistry. Adoption of heterogeneous mechanisms in cases 3 and 4 improves the agreement with measurements at the end of the AAOE mission.

We note that concentrations of ClO can be affected by the history of the air mass sampled. Although repartitioning within the active chlorine family (Cl + ClO + OClO + 2 × Cl_2O_2 + HOCl) can respond to changing illumination with a time constant of at most a few hours, partitioning between chlorine nitrate and active chlorine depends on the production of NO_x by HNO_3 photolysis, and thus changes with a time constant of about 10–30 days for latitudes higher than 70°S. Similarly, reformation of HCl through gas phase reactions has similar time constants for latitudes near 80°S.

Calculated ClO for 80°S illumination agrees better with observations at the end of the mission, even for case 1, suggesting that the temporal behavior of observations near 70°S could be explained if the sampled air parcels spent a large fraction of their previous history at latitudes near 80°S. However, latitude displacements of air parcels occur toward both north and south, resulting in, respectively, faster and slower recovery of HCl and decrease in ClO. It seems thus

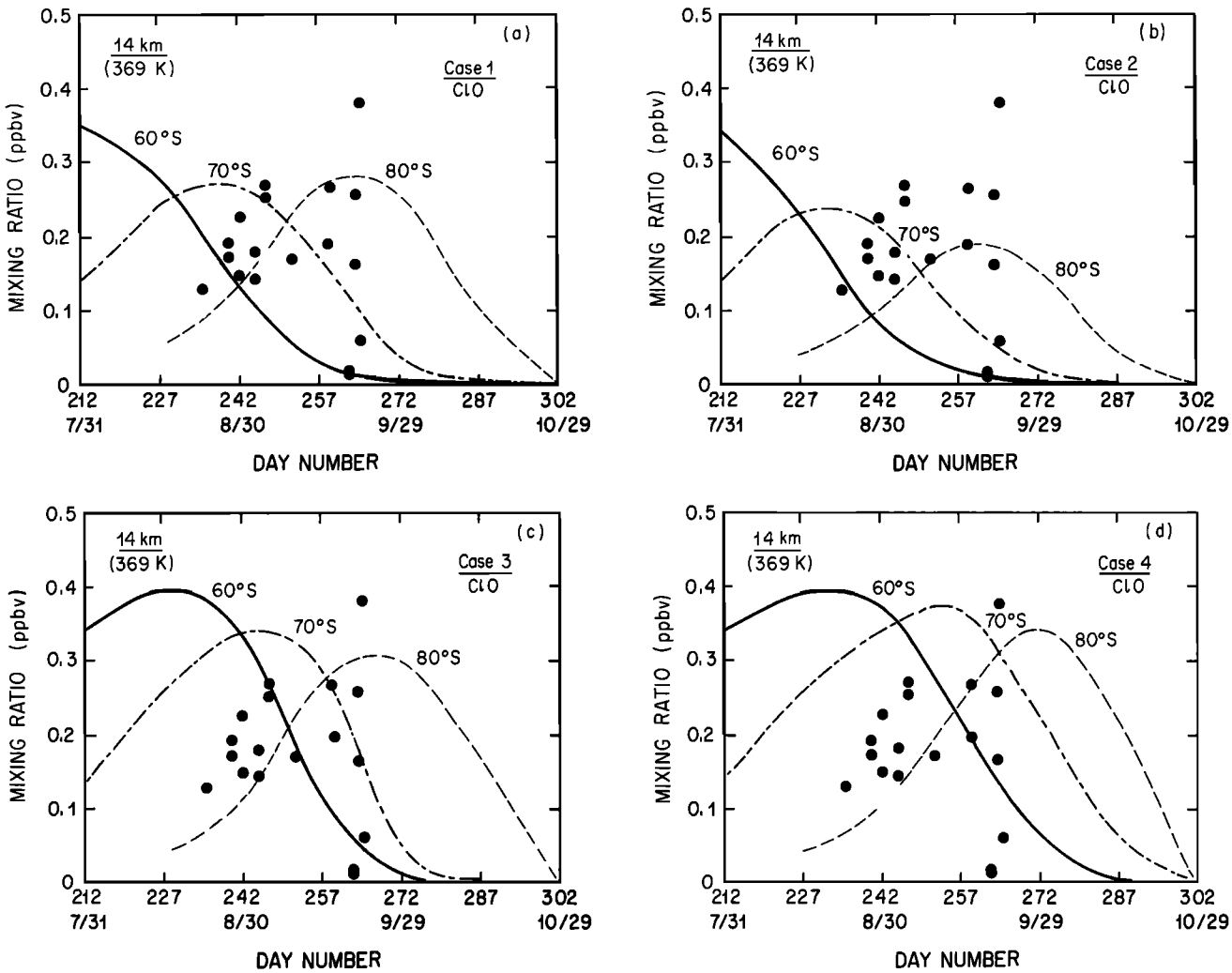

Fig. 10. Calculated mixing ratios of ClO at 14 km (369 K) for (*a*) case 1, (*b*) case 2, (*c*) case 3, and (*d*) case 4, compared with measurements by the Harvard detector on the ER-2. Data are taken from the southernmost segment of each flight (near 70°S). Calculations for different latitudes are denoted as in Figure 6.

unlikely that the trends in HCl and ClO during 1987 can be explained solely in terms of illumination history. Observations of ClO and HCl seem to require heterogeneous chemistry throughout most of September, as in case 4.

The temporal development of ClO in different years is particularly important in determining the depth of the ozone hole. As discussed by *Ko et al.* [this issue], the primary cycle for ozone removal in the Antarctic stratosphere is the Cl_2O_2 cycle (cycle III). Since the efficiency of this cycle depends on the square of the ClO concentrations, relatively small differences between different scenarios for ClO can be translated into much larger ozone reductions by the end of October. Although the ER-2 data suggest constant or increasing ClO densities until at least September 22 during 1987, ground-based observations of ClO and OClO at McMurdo in 1986 [*de Zafra et al.*, 1987; *Solomon et al.*, 1987] suggest a decrease in ClO starting in early to mid-September.

Interannual differences in the ClO trend can be due to both differences in the amount of HNO_3 left in the gas phase [*Salawitch et al.*, 1988] and in the duration of heterogeneous chemistry. Our calculations suggest that the degree of denitrification in the Antarctic stratosphere during 1987 was not sufficient to maintain high concentrations of ClO and low densities of HCl until the end of September, particularly for latitudes near 70°S. On the other hand, heterogeneous chemistry could have continued until October, since PSCs were observed by the SAM II instrument during the early part of this month. It thus seems that the long duration of heterogeneous chemistry during 1987 could be the controlling factor in maintaining high concentrations of ClO until late in the season during this year and could thus explain the extremely low ozone levels observed during October [*Ko et al.*, this issue].

The recovery of HCl could also be retarded if we had larger concentrations for OH. Concentrations of OH in Antarctica are expected to be sensitive to the rates adopted for reactions (11) and (13), concentrations of HNO_3, and methyl chemistry. No measurements of HO_x species in Antarctica exist at this point. Analysis of the temporal development of ClO and HCl data for different years, in conjunction with observations of PSCs, HNO_3, and OH could be particularly useful in determining the relative importance of heterogeneous chemistry and denitrification in controlling the behavior of HCl and ClO during September and October.

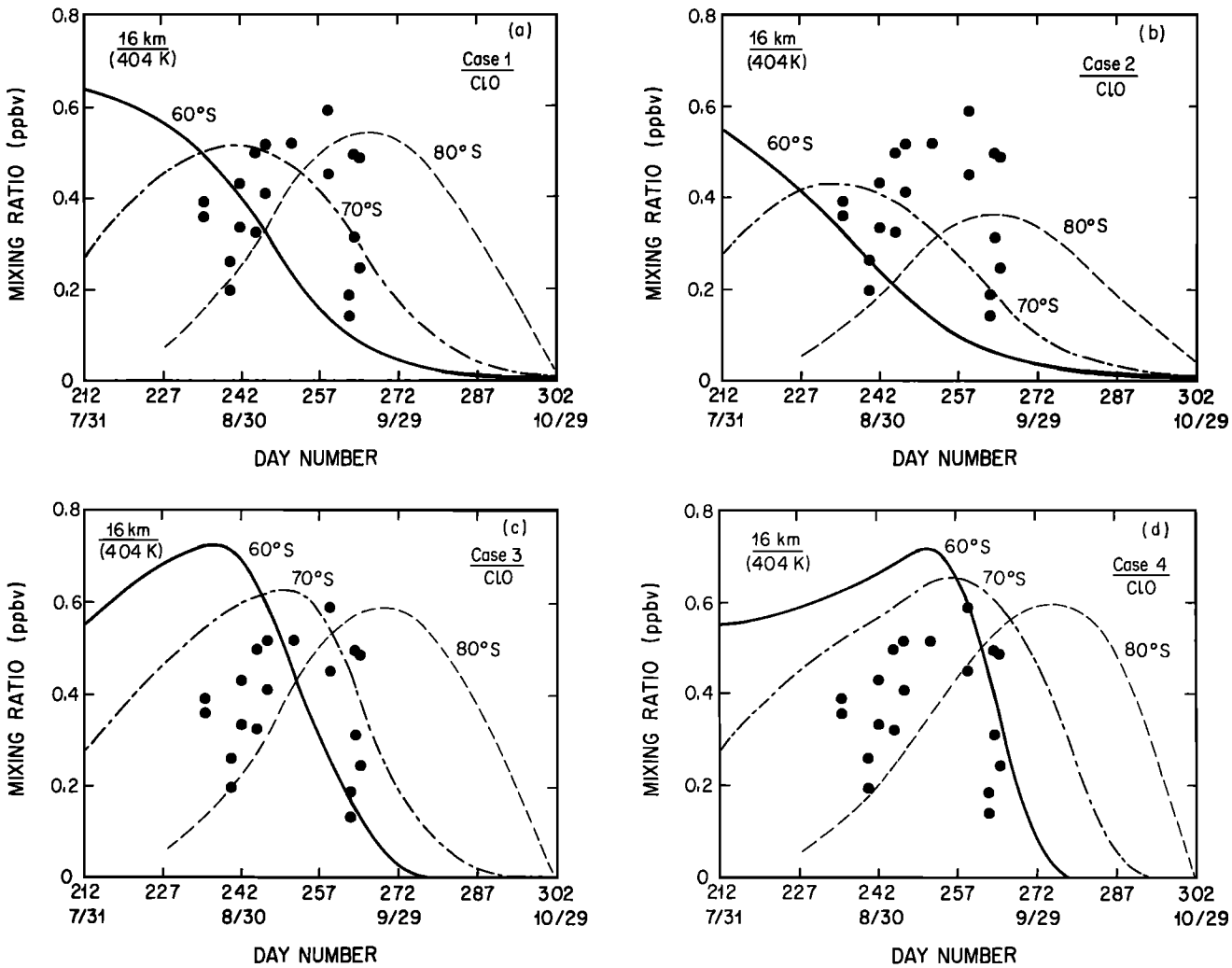

Fig. 11. Same as Figure 10, but at 16 km (404 K).

5.6. *Partitioning of Chlorine Species*

Measurements by the different AAOE instruments cannot uniquely constrain the partitioning of chlorine species as a function of altitude, since only column densities are measured for HCl and $ClNO_3$. Model calculations can be used to relate local concentrations to column densities. Such a relationship is useful in determining chlorine budgets which are consistent with observations and kinetic data.

Figure 13 shows our calculated altitude distributions for the most abundant chlorine species at noon on September 14, for the conditions of cases 1–4, 70°S. Calculated concentrations of HOCl are negligible, with column densities less than 2×10^{14} cm^{-2}, the upper bound measured by *Toon et al.* [this issue]). The abundance of $ClNO_3$ increases with altitude due to a corresponding increase in both the adopted concentration of HNO_3 (Figure 5) and its photolysis rate. The magnitude of the HCl concentration is determined by the efficiency of heterogeneous processing and is thus largest for case 1 and smallest for case 4. We note that chloride measurements by the Multifilter sampler aboard the ER-2 [*Gandrud et al.*, 1989] suggest mixing ratios of order 0.2–0.5 ppbv for HCl + $ClNO_3$ inside the vortex, consistent with case 4. Comparison of Figures 13*a*–13*d* with Figure 9 suggests that the measured column densities are consistent with HCl mixing ratios of order 0.2 ppbv. Such concentrations of HCl would require heterogeneous processing to continue into September.

The calculated partitioning of chlorine species is particularly sensitive to uncertainties in the kinetics of Cl_2O_2. As discussed in Appendix B, recent measurements of both the absorption cross section and formation rates of the ClO dimer [*Burkholder et al.*, 1988; *Sander et al.*, 1989] suggest that the calculated ClO would increase by factors of 1.4–2.0 in early September for the cases presented above. Such a revision would then suggest better agreement with observations for conditions similar to those of case 2 during this time period, thus indicating that the high column densities of $ClNO_3$ measured by DC-8 instruments in the collar region could be consistent with the in situ ClO measured aboard the ER-2. At the same time, the recovery of HCl could be accelerated by the above changes in the kinetic data (see Appendix B). Work is in progress to determine the implications of the new kinetic data for the cases discussed in this paper.

6. CONCLUSIONS

We have presented results of photochemical models for the Antarctic stratosphere during winter/spring, and com-

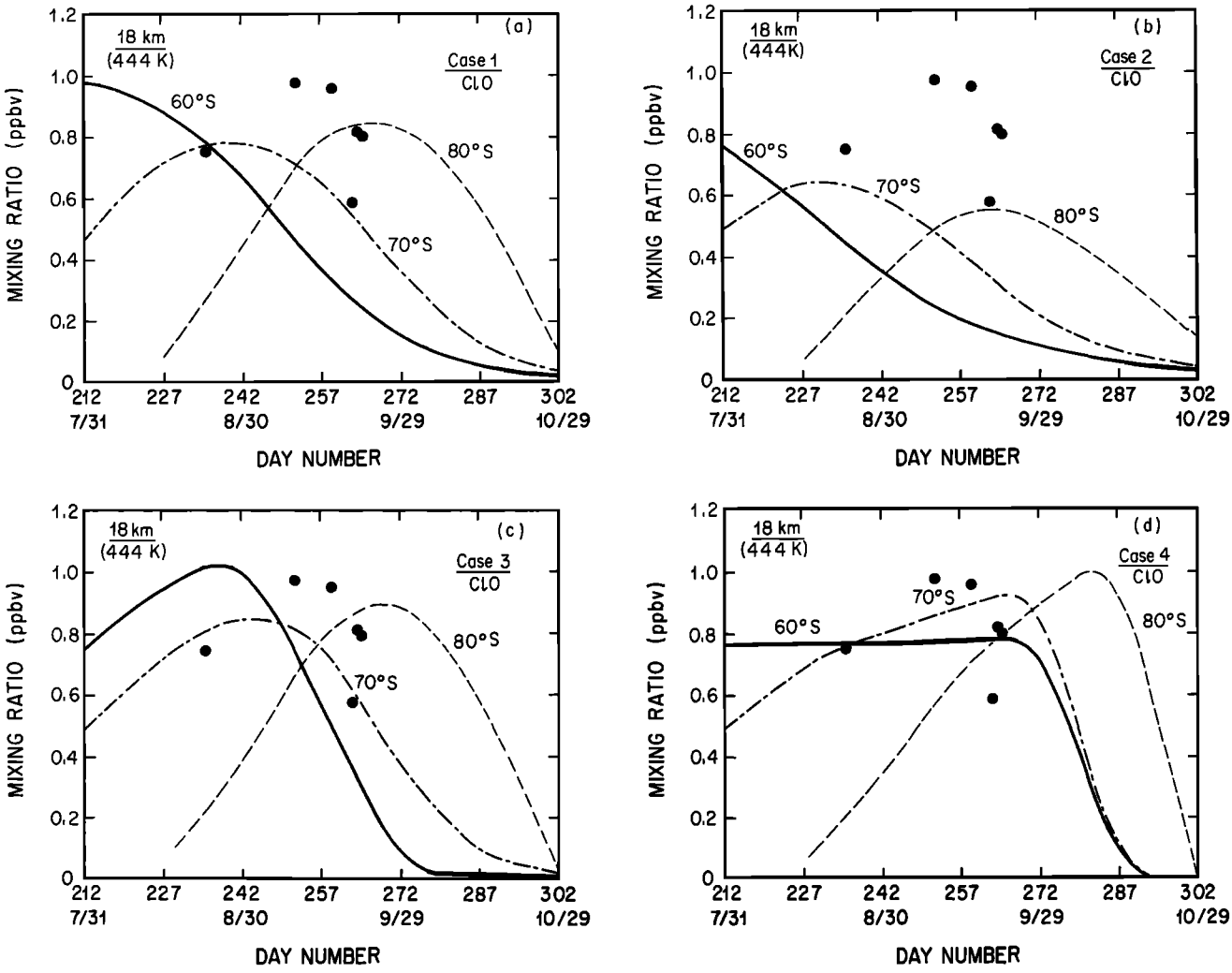

Fig. 12. Same as Figure 11, but at 18 km (444 K).

pared them with observations by the Airborne Antarctic Ozone Experiment. Since these observations were carried out only until the third week in September, photochemical models constrained by AAOE data can be used to provide extrapolation of the behavior of important species during late September and October. Such extrapolations are particularly important in ascertaining the role of chemistry in the observed ozone reductions during this period of time, as well as for past and future levels of chlorine. Implications of these model results for the behavior of ozone are discussed in a companion paper [*Ko et al.*, this issue].

Past studies indicate that the partitioning of chlorine species and the depth of the ozone hole could be very sensitive to the relative abundances of HCl and odd nitrogen prior to the onset of heterogeneous chemistry [*Wofsy et al.*, 1988], to the duration of the heterogeneous chemistry, and to the abundances of HNO_3 left in the gas phase after denitrification [*Salawitch et al.*, 1988]. We have considered four different cases, reflecting different initial amounts of odd nitrogen, and different assumptions for the importance of heterogeneous chemistry from August to October. The gas phase concentrations of HNO_3 adopted in our model have been constrained by in situ measurements of the NO_y concentrations aboard the ER-2 [*Fahey et al.*, this issue] and observations of the column density of HNO_3 aboard the DC-8 [*Toon et al.*, this issue; *Coffey et al.*, this issue]. Comparison of NO_y and HNO_3 measurements with model results suggests that 60–80% of the nitric acid has been removed from the gas phase below 20 km. Given the uncertainties in initial conditions, heterogeneous processes, and illumination history of the sampled air masses, it is difficult to consider all possibilities. We believe, however, that the cases considered here bracket the behavior of chlorine and nitrogen species in a manner consistent with AAOE observations.

The main conclusions of this study are as follows.

1. Although the amounts of chlorine nitrate and active chlorine produced by heterogeneous conversion of HCl do depend on the relative concentrations of HCl and odd nitrogen (NO_x + $ClNO_3$ + 2 × N_2O_5) prior to the appearance of PSCs [*Wofsy et al.*, 1988], the rate of heterogeneous processing of HCl is determined by the rate at which NO_x is supplied by photolysis of reservoir species or by transport. High column densities of $ClNO_3$ observed near 70°S in early September suggest that 2–3 ppbv of NO_x are supplied during August at altitudes below 22 km by either photolysis of N_2O_5 and HNO_3, or by mixing of NO_x across the vortex wall. The amount of converted HCl and the final form of

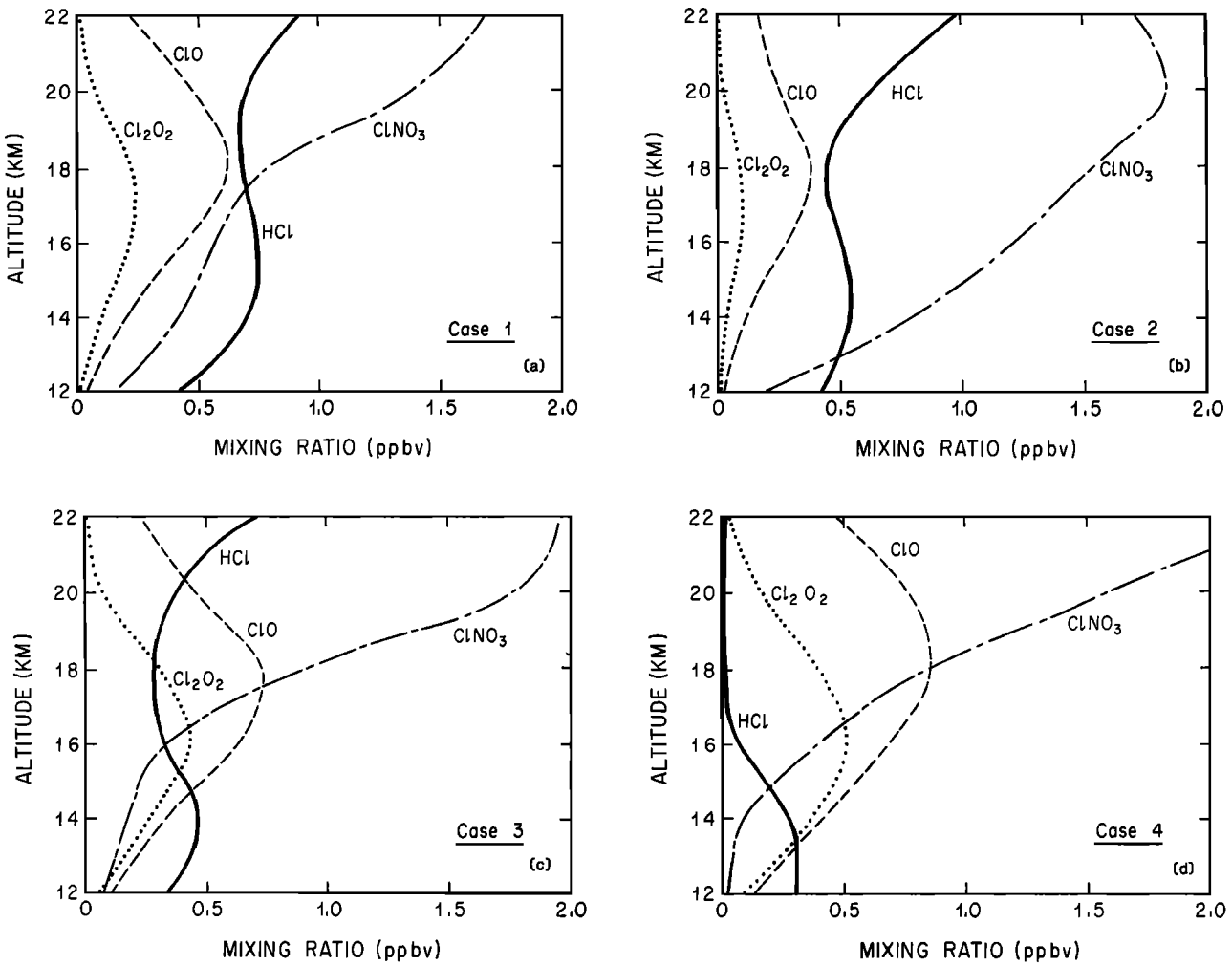

Fig. 13. Mixing ratios of HCl (solid line), $ClNO_3$ (dash-dot line), ClO (dashed line), and Cl_2O_2 (dotted line) calculated at noon, day 257 (September 14), 70°S conditions for cases (*a*) 1, (*b*) 2, (*c*) 3, and (*d*) 4.

chlorine are also sensitive to other parameters, such as the relative rates of the competing heterogeneous reactions, and the degree of illumination experienced by the air parcels during heterogeneous processing.

2. The recovery of HCl column densities calculated without heterogeneous chemistry (case 1) is faster than observations. In the absence of heterogeneous processing, photolysis of residual gas phase HNO_3 with subsequent formation of $ClNO_3$ results in rapid decrease of the calculated ClO near 70°S after the first week of September. Denitrification alone does not explain the observed temporal behavior of ClO near 70°S and of HCl. This behavior requires that heterogeneous reactions occur at substantial rates during the month of September. The long duration of PSCs during 1987 could maintain high concentrations of ClO until October and be responsible for the extremely low levels of ozone observed during that year.

The observations by the AAOE instruments are consistent with the implications of heterogeneous chemistry and the requirements of chlorine-related hypotheses for O_3 removal. Because of the sensitivity of the ozone reductions to ClO abundances through cycle III and the uncertainties in pertinent chemical mechanisms, there are still large uncertainties in how much of the ozone loss can be accounted for by chlorine chemistry [*Ko et al.*, this issue]. Furthermore, current photochemical modeling and the spatial and temporal extent of AAOE observations cannot sufficiently constrain important parameters such as the behavior of ClO during October, or the initial preconditions during early winter. Future efforts in field observations, kinetics, and atmospheric modeling should address the following issues.

1. Observations of ClO and $ClNO_3$ during August can yield important clues as to initial preconditions. Observations of ClO, $ClNO_3$, HCl, HNO_3, NO, OH, and PSCs deep in the vortex and in late September–October can clarify the relative importance of denitrification and heterogeneous chemistry in determining the seasonal and interannual behavior of ClO. Measurements of Cl_2O_2, HOCl, and N_2O_5 would supply much needed constraints to present modeling. Satellite observations of nitrogen species above 22 km can be used to determine the vertical extent of denitrification.

2. Complete processing of HCl to active chlorine during July–August seems to require that the rates of the heterogeneous reactions of $ClNO_3$ and N_2O_5 with frozen H_2O on PSC particles be substantially smaller than those for the corresponding reactions with frozen HCl. Since molar concentrations of HCl in PSC particles could be 0.1% and lower, it is important to determine the rates of reactions (10)–(13) at

these low levels of HCl. It is also important to determine the above rates in solid H_2O–HNO_3 mixtures.

3. Changes in the existing data on Cl_2O_2 absorption cross sections and formation rates will affect the calculated concentrations of trace gases. In particular, increases in the photolysis of Cl_2O_2 and reductions in its formation rate would increase the calculated ClO in early September, and accelerate the recovery of HCl. Further studies are needed on the kinetics of Cl_2O_2, particularly the formation rate at low temperatures, and determination of photolysis cross sections and photolytic products at wavelengths greater than 300 nm.

4. Photochemical modeling should also incorporate a more detailed treatment of the microphysics of aerosols and PSCs, as well as realistic estimates of the average collision frequency of gases with reacting surfaces. Such estimates can be provided by careful analysis and averaging of satellite and aircraft measurements.

5. Future photochemical modeling can profit from realistic estimates of dynamic conditions within the hole. In particular, such modeling could include possible vertical and horizontal mixing/transport, and estimates of the average illumination of ensembles of air parcels at altitudes between 12 and 24 km, and at times between July and October.

Appendix A: Parameterization of Heterogeneous Chemistry

The rate for heterogeneous reactions (10)–(13) is given by

$$K\ (\mathrm{s}^{-1}) = \nu\gamma \tag{A1}$$

where ν is the collision frequency of gas molecules with reacting surfaces and γ is the reaction efficiency per collision, sometimes referred to as the "sticking coefficient." The collision frequency ν is given by

$$\nu\ (\mathrm{s}^{-1}) = \tfrac{1}{4}\,\bar{A}\left(\frac{8kT}{\pi M}\right)^{1/2} \tag{A2}$$

where T is the temperature, M (g) the molecular weight of the gas molecules, k Boltzmann's constant, and $\bar{A}$ the reacting surface concentration per unit volume. Whereas ν can be determined from a given temperature, gas density, and aerosol size distribution, the reaction efficiency γ will also depend on the particle composition. Previous treatment of heterogeneous chemistry adopted a constant value for γ for reactions (11) and (13), while adopting a pseudo gas phase parameterization for reaction (10) [e.g., *Solomon et al.*, 1986; *Rodriguez et al.*, 1986].

Realistic parameterization of (A1) and of the rate of processing of the different species under reactions (10)–(13) requires knowledge of the following quantities: (1) surface area concentration $\bar{A}$, and relation of surface area to observed parameters such as the extinction coefficient, (2) ratio of HCl in the solid phase to HCl in the gas phase, and (3) molar fraction of HCl in the solid phase.

The relationship between surface area concentration and extinction coefficient k_{ext} (km^{-1}) is given by

$$k_{\mathrm{ext}}(\mathrm{km}^{-1}) = \frac{Q_e\bar{A}}{4}\ (\mathrm{cm}^2/\mathrm{cm}^3) \times 10^5 \tag{A3}$$

where Q_e is the extinction efficiency. We assume that the heterogeneous chemistry is occurring primarily on particles with radii 0.5 μm or greater, and thus adopt an average value of 2 for Q_e.

It is also useful to relate the surface area concentration and extinction coefficient to the amount of frozen water for a given particle radius and assumed average mass. We assume that PSC particles exhibit a composition of the form $HNO_3 \cdot jH_2O$, where a value of infinity for j would correspond to pure ice. Simple consideration of the amount of frozen mass in particles of assumed radius r_0, in conjunction with (A3), yields

$$k_{\mathrm{ext}}\ (\mathrm{km}^{-1}) = \tfrac{3}{2} \times 10^5 (f_{H_2O})(M_s)(n)\left(\frac{1+j}{j}\right)\Big/\rho r_0 \tag{A4}$$

where M_s is the average molecular weight (g) of the solid, n the background gas density, f_{H_2O} the mixing ratio of frozen water, and ρ the density of the solid (taken here as 1 g cm^{-3}). Inverting the above equation can also give the mixing ratio of frozen water for a given observed extinction coefficient, and assumed PSC radius. We thus perform calculations in which we either assume a given amount of frozen water, or adopt an observed extinction coefficient.

Calculation of the development of HCl with the heterogeneous reactions (10) and (12) must be given particular attention. Our photochemical model divides the HCl into two reservoirs: solid and gas. Gas phase photochemical losses are assumed to act only on the gas phase reservoir, while loss through reactions (10) and (12) is effective on the solid reservoir. Production of HCl by gas phase reactions contributes to both reservoirs according to the assumed solid gas equilibrium. Both phases are adjusted to equilibrium conditions at each time step of the calculation. We assume that gas phase partial pressures p_{HCl} and solid phase molar ratios m_{HCl} are related by [*Wofsy et al.*, 1988]

$$(m_{\mathrm{HCl}})^2 = Hp_{\mathrm{HCl}} \tag{A5}$$

The proportionality constant above at pressure p is given by

$$H = \frac{p(m^0 f_{H_2O})^2}{p^0} \tag{A6}$$

where f_{H_2O} is the mixing ratio of water in the solid and m^0 is the molar ratio of HCl in equilibrium with a partial pressure p^0 of HCl for temperatures typical of the lower stratosphere. We assume values of 0.02 mol/mol and 10^{-7} torrs for m^0 and p^0, respectively, from the estimates of *Wofsy et al.* [1988]. (Recent measurements by *Hanson and Mauersberger* [1988] indicate that these values are reasonable for nitric acid trihydrates but about a factor of 10 too large for pure ice.) Since these values are very uncertain at this point, we have not taken into consideration temperature changes within the altitude region of interest. Equations (A5) and (A6) in conjunction with mass balance considerations are used to derive the fraction of HCl in the solid phase, and the molar fraction of this HCl.

Recent kinetic data suggest that the rates of (10)–(13) depend on the molar fraction of HCl in a nonlinear manner [*Molina et al.*, 1987; *Tolbert et al.*, 1987; *Leu*, 1988*a*, *b*]. In particular, the reaction efficiency of (10) is fairly constant at high molar ratios of HCl, with (11) seemingly negligible under these conditions. At lower molar fractions, both (10) and (11) seem to be operative, with a total reaction efficiency which depends on the HCl concentration [*Leu*, 1988*a*]. A

similar behavior seems to occur for (12) and (13) [*Leu*, 1988*b*]. We note, however, that uncertainties in the detection of products such as HOCl or $ClNO_2$ preclude at present the accurate determination of the relative rates of (10)–(13) for large molar fractions of HCl.

Our calculations assume the following simplified behavior for (10)–(13).

1. The reaction efficiencies for (10) and (12) are assumed to be constant down to a given molar fraction m, and proportional to the molar fraction for values below m. The value of m is taken to be 0.0 in the period before August 1, and 0.01 thereafter.

2. The reaction efficiencies for (11) and (13) are assumed to be zero for molar fractions greater than m', and constant for values below m'. The value of m' is the same as the value of m above, unless otherwise specified.

These assumptions result in efficient processing of HCl during July–August (see section 3). We must stress that the above assumptions for (10)–(13), although consistent with existing data, still have to be substantiated by laboratory experiments.

Appendix B: Sensitivity to Kinetics of the ClO Dimer

The formation and photolysis rates of Cl_2O_2 play a crucial role in the modeling of the Antarctic stratosphere. Reports of recent measurements [*Burkholder et al.*, 1988; *Sander et al.*, 1989] indicate that the photolysis and formation rate of Cl_2O_2 are larger and smaller, respectively, than the values used in this study by factors of 2–3. A complete assessment of the impact of these new data will be the subject of a forthcoming publication. This appendix presents simple algebraic formulas allowing us to estimate the impact of changes in the above rates on the calculated partitioning between ClO and Cl_2O_2. We also use these formulas to indicate the effect of the above rates on the calculated recovery of HCl.

The photolysis rates of Cl_2O_2 adopted in this study yield lifetimes of less than 1 hour near 70°S for the ClO dimer during the AAOE period. The partitioning between ClO and Cl_2O_2 at noon is then given approximately by the equilibrium between the reactions

$$ClO + ClO + M \rightarrow Cl_2O_2 + M \ (k_1) \qquad (B1)$$

$$Cl_2O_2 + h\nu \rightarrow 2 \times ClO \ (J_2) \qquad (B2)$$

where the products in (B2) reflect the rapid conversion to ClO of the different photolytic products of Cl_2O_2.

We define a quantity C equal to the total amount of chlorine in ClO and its dimer,

$$C = [ClO] + 2 \times [Cl_2O_2] \qquad (B3)$$

In particular, we note that

$$C \sim ClY - ([ClNO_3] + [HCl]) \qquad (B4)$$

since other chlorine reservoir species are negligible during the AAOE period. The daytime equilibrium of (B1) and (B2) implies that

$$[Cl_2O_2] = (k_1[M][ClO]^2)/J_2 \qquad (B5)$$

Combining (B5) and (B3), we obtain a quadratic equation for [ClO] with solution

$$[ClO] = J_2\left\{\left(1 + \frac{8k_1[M]C}{J_2}\right)^{1/2} - 1\right\}/(4k_1[M]) \qquad (B6)$$

Equation (B6) can be used to estimate the ClO abundance for a given set of kinetic data if we know the abundance of C. Equation (B3) can then be used to calculate Cl_2O_2.

The calculated abundance of C for cases 1–4 is not very sensitive to changes in the dimer kinetics until HCl starts to recover in September. Formation of HCl and $ClNO_3$ during this month will then reduce the magnitude of C by factors of 10–100. The recovery of HCl is determined by production through the reaction

$$Cl + CH_4 \rightarrow HCl + CH_3 \qquad (B7)$$

as well as by loss through

$$OH + HCl \rightarrow Cl + H_2O \qquad (B8)$$

$$ClNO_3 + HCl \text{ (ice)} \rightarrow Cl_2 + HNO_3 \text{ (ice)} \qquad (B9)$$

Reaction (B8) is negligible, to first order, for the OH densities calculated within the vortex during the AAOE period in our model. We note that in the absence of substantial amounts of NO, the concentration of Cl is determined by production through the photolysis of Cl_2O_2, and loss through the reaction

$$Cl + O_3 \rightarrow ClO + O_3 \ (k_{10}) \qquad (B10)$$

The concentration of Cl is then approximately given by

$$[Cl] \sim (2J_2[Cl_2O_2])/(k_{10}[O_3]) \qquad (B11)$$

Changes in the kinetics of Cl_2O_2 will then also affect the rate of recovery of HCl, and thus the calculated temporal behavior of C during September.

We can expand (B6) in a Taylor series for the following conditions.

1. $C \gg J_2/8k_1[M]$: this condition holds in general during late August to early September, before the recovery of HCl sets in. We have

$$[ClO] \sim 2C(J_2/8k_1[M]C)^{1/2} \qquad (B12)$$

$$[Cl_2O_2] \sim C\{0.5 - (J_2/8k_1[M]C)^{1/2}\} \qquad (B13)$$

In this case, most of the C is in the form of Cl_2O_2. The ClO concentrations vary directly and inversely as the square root of the photolysis and formation rates of Cl_2O_2, respectively. Furthermore, the concentrations of Cl, and thus the rate of recovery of HCl, vary almost linearly with the photolysis of Cl_2O_2.

2. $C \ll J_2/8k_1[M]$: this condition will hold in middle to late September, when a substantial amount of HCl has been reformed. In this case, expansion of (B6) yields

$$[ClO] \sim C(1 - 2k_1[M]C/J_2) \qquad (B14)$$

$$[Cl_2O_2] \sim k_1[M]C^2/J_2 \qquad (B15)$$

In this case, most of the C is in the form of ClO. Concentrations of ClO are then fairly independent of the dimer kinetics. The recovery rate of HCl is then insensitive to

changes in the photolysis rate of Cl_2O_2 but will respond to changes in the formation rate.

We may then expect the following changes in the calculated ClO and HCl as a result of the reported increase/decrease in the photolysis/formation rate of Cl_2O_2. Calculated concentrations of ClO increase by factors of 1.4–2.0 during late August to early September. At the same time, the HCl recovery will set in earlier. As a result, calculated concentrations of C and ClO for mid-September will be reduced. We also note that, since the catalytic removal of O_3 is also proportional to $J_2 \times [Cl_2O_2]$ [*Ko et al.*, this issue], ozone reductions will occur at a faster rate during late August to early September.

Acknowledgments. S. Robert Orfeo facilitated the implementation of this project within its critical time frame. We acknowledge stimulating discussions with Mack McFarland and Robert Watson. Steve Walker played a key role in setting up AER's computer resources in Punta Arenas. Daniel Murphy, Richard Winkler, and Mark Schoeberl provided us with much of the ER-2 data in unified form. We would also like to thank the referees for their valuable comments. This work has been supported by the Fluorocarbon Program Panel of the Chemical Manufacturers Association, and by the Upper Atmospheric Theory and Data Analysis Program of NASA.

REFERENCES

Austin, J., R. R. Garcia, J. M. Russell III, S. Solomon, and A. F. Tuck, On the atmospheric photochemistry of nitric acid, *J. Geophys. Res.*, *91*, 5477–5485, 1986.

Austin, J., et al., Lagrangian photochemical modeling studies of the 1987 Antarctic spring vortex, 2, Seasonal trends in ozone, *J. Geophys. Res.*, this issue.

Baldwin, A. C., and D. M. Golden, Heterogeneous atmospheric reactions: Sulfuric acid aerosols as tropospheric sinks, *Science*, *206*, 562, 1979.

Bojkov, R. D., The 1979–1985 ozone decline in the Antarctic as reflected in ground based observations, *Geophys. Res. Lett.*, *13*, 1236–1239, 1986.

Brune, W. H., J. G. Anderson, and K. R. Chan, In situ observations of ClO in the Antarctic: ER-2 aircraft results from 54°S to 72°S latitude, *J. Geophys. Res.*, this issue.

Burkholder, J. B., J. J. Orlando, P. D. Hammer, and C. J. Howard, Measurements of the ClO radical vibrational band intensity and the ClO + ClO + M reaction product (abstract), *NASA Conf. Publ.*, *10014*, 1988.

Callis, L. B., and M. Natarajan, The Antarctic ozone minimum: Relationship to odd nitrogen, odd chlorine, the final warming, and the 11-year solar cycle, *J. Geophys. Res.*, *91*, 10,771–10,796, 1986.

Chan, K. R., S. G. Scott, T. P. Bui, S. W. Bowen, and J. Day, Temperature and horizontal wind measurements on the ER-2 aircraft during the 1987 Airborne Antarctic Ozone Experiment, *J. Geophys. Res.*, *94*, 11,573–11,587, 1989.

Chubachi, S., Preliminary result of ozone observations at Syowa Station from February 1982 to January 1983, *Mem. Natl. Inst. Polar Res. Spec. Issue Jpn.*, *34*, 13, 1984.

Chubachi, S., On the cooling of stratospheric temperature at Syowa, Antarctica, *Geophys. Res. Lett.*, *13*, 1221–1223, 1986.

Coffey, M. T., Mankin, W. G., and A. Goldman, Airborne measurements of stratospheric constituents over Antarctica in the austral spring 1987, 2, Halogen and nitrogen trace gases, *J. Geophys. Res.*, this issue.

Crutzen, P. J., and F. Arnold, Nitric acid cloud formation in the cold antarctic stratosphere: A major cause for the springtime "ozone hole," *Nature*, *324*, 651, 1986.

de Zafra, R. L., M. Jaramillo, A. Parrish, P. Solomon, B. Connor, and J. Barrett, Observations of abnormally high concentrations of chlorine monoxide at low altitude in the antarctic spring stratosphere, I, Diurnal variation, *Nature*, *328*, 408, 1987.

de Zafra, R. L., M. Jaramillo, J. Barrett, L. K. Emmons, P. M. Solomon, and A. Parrish, New observations of a large concentration of ClO in the springtime lower stratosphere over Antarctica and its implications for ozone-depleting chemistry, *J. Geophys. Res.*, *94*, 11,423–11,428, 1989.

Fahey, D. W., D. M. Murphy, C. S. Eubank, K. Kelly, M. H. Proffitt, G. V. Ferry, M. K. W. Ko, M. Loewenstein, and K. R. Chan, Measurements of nitric oxide and total reactive nitrogen in the Antarctic stratosphere: Observations and chemical implications, *J. Geophys. Res.*, this issue.

Farman, J. C., B. G. Gardiner, and J. D. Shanklin, Large losses of total ozone in Antarctica reveal seasonal Cl_x/NO_x interaction, *Nature*, *315*, 207, 1985.

Farmer, C. B., G. C. Toon, P. W. Shaper, J. F. Blavier, and L. L. Lowes, Ground-based measurements of the composition of the antarctic atmosphere during the 1986 spring season, I, Stratospheric trace gases, *Nature*, *329*, 126, 1987.

Friedl, R. R., J. H. Goble, and S. P. Sander, A kinetics study of the homogeneous and heterogeneous components of the HCl + $ClONO_2$ reaction, *Geophys. Res. Lett.*, *13*, 1351–1354, 1986.

Gandrud, B. W., P. D. Sperry, and L. Sanford, Filter measurements of chemical composition during the Airborne Antarctic Ozone Experiment (abstract), *NASA Conf. Publ.*, *10014*, 1988.

Gandrud, B. W., P. D. Sperry, L. Sanford, K. K. Kelly, G. V. Ferry, and K. R. Chan, Filter measurement results from the Airborne Antarctic Ozone Experiment, *J. Geophys. Res.*, *94*, 11,285–11,297, 1989.

Hanson, D., and K. Mauersberger, Solubility and equilibrium vapor pressures of HCl dissolved in polar stratospheric cloud materials: Ice and the trihydrate of nitric acid, *Geophys. Res. Lett.*, *15*, 1507–1510, 1988.

Harker, A. B., and D. R. Strauss, Kinetics of the heterogeneous hydrolysis of dinitrogen pentoxide over the temperature range 214–263°K, *Rep. FAA-EE-81-3*, Fed. Aviat. Admin., Washington, D. C., 1981.

Hartmann, D. L., L. E. Heidt, M. Loewenstein, J. R. Podolske, J. F. Vedder, W. L. Starr, and S. E. Strahan, Transport into the south polar vortex in early spring, *J. Geophys. Res.*, this issue.

Hayman, G. D., J. M. Davies, and R. A. Cox, Kinetics of the reaction ClO + ClO → products and its potential relevance to Antarctic ozone, *Geophys. Res. Lett.*, *13*, 1347–1350, 1986.

Heidt, L. E., J. F. Vedder, W. H. Pollock, R. A. Lueb, and B. E. Henry, Trace gases in the Antarctic atmosphere, *J. Geophys. Res.*, *94*, 11,599–11,611, 1989.

Hofmann, D. J., J. M. Rosen, J. W. Harder, and S. R. Rolf, Ozone and aerosol measurements in the springtime Antarctic stratosphere in 1985, *Geophys. Res. Lett.*, *13*, 1252–1255, 1986.

Hofmann, D. J., J. W. Harder, S. R. Rolf, and J. M. Rosen, Balloon-borne observations of the development and vertical structure of the Antarctic ozone hole in 1986, *Nature*, *326*, 59–62, 1987.

Jones, R. J., et al., Lagrangian photochemical modeling studies of the 1987 Antarctic spring vortex: Comparison with AAOE observations, *J. Geophys. Res.*, *94*, 11,529–11,558, 1989.

Kelly, K. K., et al., Dehydration in the lower Antarctic stratosphere during late winter and early spring 1987, *J. Geophys. Res.*, *94*, 11,317–11,357, 1989.

Ko, M. K. W., K. K. Tung, D. K. Weisenstein, and N. D. Sze, A zonal-mean model of stratospheric tracer transport in isentropic coordinates: Numerical simulations for nitrous oxide and nitric acid, *J. Geophys. Res.*, *90*, 2313, 1985.

Ko, M. K. W., J. M. Rodriguez, N. D. Sze, M. H. Proffitt, W. L. Starr, A. J. Krueger, E. V. Browell, and M. P. McCormick, Implications of Airborne Antarctic Ozone Experiment observations for proposed chemical explanations of the seasonal and interannual behavior of Antarctic ozone, *J. Geophys. Res.*, this issue.

Krueger, A. J., M. R. Schoeberl, and R. S. Stolarski, TOMS observations of total ozone in the 1986 Antarctic spring, *Geophys. Res. Lett.*, *14*, 527–530, 1987.

Leu, M.-T., Laboratory studies of sticking coefficients and heterogeneous reactions important in the Antarctic stratosphere, *Geophys. Res. Lett.*, *15*, 17–20, 1988*a*.

Leu, M.-T., Heterogeneous reactions of N_2O_5 with H_2O and HCl on ice surfaces: Implications for Antarctic ozone depletion, *Geophys. Res. Lett.*, *15*, 851–854, 1988*b*.

Mahlman, J. D., and S. B. Fels, Antarctic ozone decreases: A dynamical cause?, *Geophys. Res. Lett.*, *13*, 1316–1319, 1986.

Mankin, W. G., and M. T. Coffey, Airborne measurements of

stratospheric constituents over Antarctica in the austral spring 1987: Method and ozone observations, *J. Geophys. Res.*, *94*, 11,413–11,421, 1989.

Martin, L. R., H. S. Judeikis, and M. Wu, Heterogeneous reactions of Cl and ClO in the stratosphere, *J. Geophys. Res.*, *85*, 5511–5518, 1980.

McCormick, M. P., and J. C. Larsen, Antarctic springtime measurements of ozone, nitrogen dioxide, and aerosol extinction by SAM II, SAGE, and SAGE II, *Geophys. Res. Lett.*, *13*, 1280–1283, 1986.

McElroy, M. B., R. J. Salawitch, S. C. Wofsy, and J. A. Logan, Antarctic ozone: Reductions due to synergistic interactions of chlorine and bromine, *Nature*, *321*, 759, 1986*a*.

McElroy, M. B., R. J. Salawitch, and S. C. Wofsy, Antarctic O_3: Chemical mechanisms for the spring decrease, *Geophys. Res. Lett.*, *13*, 1296–1299, 1986*b*.

McElroy, M. B., R. J. Salawitch, and S. C. Wofsy, Chemistry of the Antarctic stratosphere, *Planet. Space Sci.*, *36*, 73–87, 1988.

Molina, L. T., and M. J. Molina, Production of Cl_2O_2 by the self reaction of the ClO radical, *J. Phys. Chem.*, *91*, 433, 1987.

Molina, L. J., T. L. Tso, L. T. Molina, and F. C. Y. Wang, Antarctic stratospheric chemistry of chlorine nitrate, hydrogen chloride and ice: Release of active chlorine, *Science*, *238*, 1253, 1987.

Mount, G. H., R. W. Sanders, A. L. Schmeltekopf, and S. Solomon, Visible spectroscopy of McMurdo Station, Antarctica, 1, Overview and daily variations of NO_2 and O_3 during austral spring 1986, *J. Geophys. Res.*, *92*, 8320–8328, 1987.

Mozurkewich, M., and J. G. Calvert, Reaction probability of N_2O_5 on aqueous aerosols, *J. Geophys. Res.*, *93*, 15,889–15,896, 1988.

NASA, Present state of knowledge of the upper atmosphere 1988: An assessment report, Report from R. J. Watson and Ozone Trends Panel, M. J. Prather and Ad Hoc Theory Panel, and M. J. Kurylo and NASA Panel for Data Evaluation, *NASA Ref. Publ.*, *1208*, Aug. 1988.

NASA Panel for Data Evaluation, Chemical kinetics and photochemical data for use in stratospheric modeling, Evaluation no. 8, *JPL Publ.*, *87-41*, 1987.

Poole, L. R., and M. P. McCormick, Polar stratospheric clouds and the Antarctic ozone hole, *J. Geophys. Res.*, *93*, 8423–8430, 1988.

Proffitt, M. H., M. J. Steinkamp, J. A. Powell, R. J. McLaughlin, O. A. Mills, A. L. Schmeltekopf, T. L. Thompson, A. F. Tuck, T. Tyler, R. H. Winkler, and K. R. Chan, In situ measurements within the 1987 Antarctic ozone hole from a high-altitude ER-2 aircraft, *J. Geophys. Res.* this issue.

Rodriguez, J. M., M. K. W. Ko, and N. D. Sze, Chlorine chemistry in the Antarctic stratosphere: Impact of OClO and Cl_2O_2 and implications for observations, *Geophys. Res. Lett.*, *13*, 1292–1295, 1986.

Rossi, M. J., R. Malhotra, and D. M. Golden, Heterogeneous chemical reaction of chlorine nitrate and water on sulfuric acid surfaces at room temperature, *Geophys. Res. Lett.*, *14*, 127–130, 1987.

Salawitch, R. J., S. C. Wofsy, and M. B. McElroy, Influence of polar stratospheric clouds on the depletion of Antarctic ozone, *Geophys. Res. Lett.*, *15*, 871–874, 1988.

Sander, S. P., and R. R. Friedl, Kinetics and product studies of the BrO + ClO reaction: Implications for Antarctic chemistry, *Geophys. Res. Lett.*, *15*, 887–890, 1988.

Sander, S. P., R. R. Friedl, and Y. L. Yung, Rate for formation of the ClO dimer in the polar stratosphere: Implications for ozone loss, *Science*, *245*, 1095–1098, 1989.

Sanders, R. W., S. Solomon, M. A. Carroll, and A. L. Schmeltekopf, Visible and near-ultraviolet spectroscopy at McMurdo Station, Antarctica, 4, Overview and daily measurements of NO_2, O_3, and OClO during 1987, *J. Geophys. Res.*, *94*, 11,381–11,391, 1989.

Solomon, P., B. Connor, R. de Zafra, A. Parrish, J. Barrett, and M. Jaramillo, Observations of abnormally high concentrations of chlorine monoxide at low altitudes in the antarctic spring stratosphere, II, Secular variation, *Nature*, *328*, 411, 1987.

Solomon, S., R. R. Garcia, F. S. Rowland, and D. J. Wuebbles, On the depletion of antarctic ozone, *Nature*, *321*, 755, 1986.

Solomon, S., G. H. Mount, R. W. Sanders, and A. L. Schmeltekopf, Visible spectroscopy at McMurdo station, Antarctica, 2, Observations of OClO, *J. Geophys. Res.*, *92*, 8329, 1987.

Solomon, S., R. W. Sanders, M. A. Carroll, and A. L. Schmeltekopf, Visible and near-ultraviolet spectroscopy at McMurdo Station, Antarctica, 5, Observations of the diurnal variations of BrO and OClO, *J. Geophys. Res.*, *94*, 11,393–11,403, 1989.

Starr, W. L., and J. F. Vedder, Measurements of ozone in the Antarctic atmosphere during August and September 1987, *J. Geophys. Res.*, *94*, 11,449–11,463, 1989.

Steele, H. M., P. Hamill, M. P. McCormick, and T. J. Swissler, The formation of polar stratospheric clouds, *J. Atmos. Sci.*, *40*, 2055, 1983.

Stolarski, R. S., A. J. Krueger, M. R. Schoeberl, R. D. McPeters, P. A. Newman, and J. C. Alpert, Nimbus 7 satellite measurements of the springtime antarctic ozone decrease, *Nature*, *322*, 808, 1986.

Tolbert, M. A., M. J. Rossi, R. Malhotra, and D. M. Golden, Reaction of chlorine nitrate with hydrogen chloride and water at Antarctic stratospheric temperatures, *Science*, *238*, 1258, 1987.

Tolbert, M. A., M. J. Rossi, and D. M. Golden, Heterogeneous chemistry related to Antarctic ozone depletion chemistry: Reactions of N_2O_5 with H_2O and HCl on ice surfaces, *Science*, *240*, 1018–1021, 1988*a*.

Tolbert, M. A., M. J. Rossi, and D. M. Golden, Heterogeneous interactions of chlorine nitrate, hydrogen chloride, and nitric acid with sulfuric acid surfaces at stratospheric temperatures, *Geophys. Res. Lett.*, *15*, 847–850, 1988*b*.

Toon, G. C., C. B. Farmer, L. L. Lowes, P. W. Schaper, J.-F. Blavier, and R. H. Norton, Infrared aircraft measurements of stratospheric composition over Antarctica during September 1987, *J. Geophys. Res.*, this issue.

Toon, O. B., P. Hamill, R. P. Turco, and J. Pinto, Condensation of HNO_3 and HCl in the winter polar stratosphere, *Geophys. Res. Lett.*, *13*, 1284–1287, 1986.

Toon, O. B., R. P. Turco, J. Jordan, J. Goodman, and G. Ferry, Physical processes in polar stratospheric ice clouds, *J. Geophys. Res.*, *94*, 11,359–11,380, 1989.

Tuck, A. F., Synoptic and chemical evolution of the Antarctic vortex in late winter an early spring 1987, *J. Geophys. Res.*, *94*, 11,687–11,737, 1989.

Tung, K. K., M. K. W. Ko, J. M. Rodriguez, and N. D. Sze, Are antarctic ozone variations a manifestation of dynamics or chemistry?, *Nature*, 322, 811–813, 1986.

Turco, R. F., O. B. Toon, and P. Hamill, Heterogeneous physicochemistry of the polar ozone hole, *J. Geophys. Res.*, this issue.

Wahner, A., R. O. Jakoubek, G. H. Mount, A. R. Ravishankara, and A. L. Schmeltekopf, Remote sensing observations of daytime column NO_2 during the Airborne Antarctic Ozone Experiment, August 22 to October 2, 1987, *J. Geophys. Res.*, this issue.

Wofsy, S. C., M. J. Molina, R. J. Salawitch, L. E. Fox, and M. B. McElroy, Interactions between HCl, NO_x, and H_2O ice in the Antarctic stratosphere: Implications for ozone, *J. Geophys. Res.*, *93*, 2442–2450, 1988.

Worsnop, D., M. Zahniser, C. Kolb, L. Watson, J. Van Doren, J. Jayne, and P. Davidovits, Mass accommodation coefficient measurements for HNO_3, HCl and N_2O_5 on water, ice and aqueous sulfuric acid droplet surfaces (abstract), *NASA Conf. Publ.*, *10014*, 1988.

J. G. Anderson, Harvard University, Cambridge, MA 02139.

K. R. Chan, W. L. Starr, and J. F. Vedder, NASA Ames Research Center, Moffett Field, CA 94035.

M. T. Coffey, L. E. Heidt, and W. G. Mankin, National Center for Atmospheric Research, Boulder, CO 80307.

D. W. Fahey and K. Kelly, NOAA Aeronomy Laboratory, Boulder, CO 80303.

C. B. Farmer and G. C. Toon, Jet Propulsion Laboratory, Pasadena, CA 91109.

M. P. McCormick, NASA Langley Research Center, Hampton, VA 23665.

M. K. W. Ko, S. D. Pierce, N. D. Sze, and J. M. Rodriguez, Atmospheric and Environmental Research, Inc., 840 Memorial Drive, Cambridge, MA 02139.

(Received May 11, 1988;
revised April 18, 1989;
accepted April 18, 1989.)